Journal of Archaeological Science 161 (2024) 105897

Contents lists available at ScienceDirect

Journal of Archaeological Science

journal homepage: www.elsevier.com/locate/jas

Searching for traces of human activity in earthen floor sequences: high-resolution geoarchaeological analyses at an Early Iron Age village in Central Iberia

Laura Tomé [a,b,*], Eneko Iriarte [c], Antonio Blanco-González [d], Margarita Jambrina-Enríquez [a,e], Natalia Égüez [a,b], Antonio V. Herrera-Herrera [a,f], Carolina Mallol [a,b,g]

[a] Archaeological Micromorphology and Biomarkers Laboratory (AMBI Lab), Instituto Universitario de Bio-Orgánica "Antonio González", Universidad de La Laguna, 38206, Tenerife, Spain
[b] Área de Prehistoria, Departamento de Geografía e Historia, Facultad de Humanidades, Universidad de La Laguna, 38206, Tenerife, Spain
[c] Área de Paleontología, Departamento de Historia, Geografía y Comunicación, Facultad de Humanidades y Comunicación, Universidad de Burgos, 09001, Burgos, Spain
[d] Research Group PREHUSAL, Departamento de Prehistoria, Historia Antigua y Arqueología, Facultad de Geografía e Historia, Universidad de Salamanca, 37002, Salamanca, Spain
[e] Área de Petrología y Geoquímica, Departamento de Biología Animal, Edafología y Geología, Facultad de Ciencias, Universidad de La Laguna, 38200, Tenerife, Spain
[f] Departamento de Química, Unidad Departamental de Química Analítica, Facultad de Ciencias, Universidad de La Laguna, 38206, Tenerife, Spain
[g] Interdisciplinary Center for Archaeology and the Evolution of Human Behaviour (ICArEHB), Universidade do Algarve, Campus de Gambelas, Edifício 1, 8005-139, Faro, Portugal

ARTICLE INFO

Keywords:
Geoarchaeology
Micromorphology
Lipid biomarkers
Iron age
Household archaeology
Earthen architecture

ABSTRACT

The Northern Iberian Plateau during the Early Iron Age witnessed the proliferation of villages, showcasing well-preserved earthen architectural remains that offer valuable insights into past daily life practices. However, the application of high-resolution geoarchaeological approaches to these contexts has been largely overlooked, despite their significance in assessing complex sedimentary sequences predominantly composed of earth-based construction materials. This paper presents the outcomes of a microcontextual geoarchaeological study conducted on earthen dwellings from the Early Iron Age village of Cerro de San Vicente (Salamanca, Northern Iberia). Our study employed soil micromorphology, lipid biomarker analysis, XRD, and XRF analyses to investigate site formation processes, characterize construction materials and techniques, and explore aspects of daily life practices, functionality, and dwelling life histories. Our results have enabled the identification of three distinct construction layers within the dwellings, shedding light on recurrent events of floor use, maintenance, and repaving. Additionally, we have detected periods of abandonment and decay of the earth-based construction material that inform on the dynamics of abandonment and reuse within the village. Furthermore, our analysis has revealed the presence of well-preserved lipid biomarkers throughout the sequences, possibly associated with the past functionality of the dwellings. Ongoing and future analyses will further contribute to our understanding of ancient construction practices and the utilization of domestic spaces at Cerro de San Vicente. This study significantly enhances the limited availability of high-resolution, microcontextual data sets concerning Iron Age contexts in Iberia, underscoring the potential of our approach for future consolidation and advancement. By combining different geoarchaeological methodologies, we demonstrate the importance of integrating diverse analytical techniques to gain comprehensive insights into the socio-cultural dynamics of the Early Iron Age settlements.

1. Introduction

The Early Iron Age (*ca.* 900–400 BCE) (henceforth EIA) in Iberia involves a mosaic of diverging regional cultural trajectories (Cunliffe and Keay, 1995; Ruiz Zapatero et al., 2020). So far, archaeological research has primarily focused on coastal settings, where the presence of

* Corresponding author. Archaeological Micromorphology and Biomarkers Laboratory (AMBI Lab), Instituto Universitario de Bio-Orgánica "Antonio González", Universidad de La Laguna, 38206, Tenerife, Spain.
E-mail address: lhernant@ull.edu.es (L. Tomé).

https://doi.org/10.1016/j.jas.2023.105897
Received 25 August 2023; Received in revised form 5 November 2023; Accepted 7 November 2023
Available online 22 November 2023

Mediterranean traders and settlers is well documented (Dietler and López-Ruiz, 2009). These Iberian settings have provided relevant data to current debates on Iron Age Europe, such as the emergence of a wide-scale interconnected Mediterranean and the resurgence of regional and local cultural identities (Hodos, 2020). However, the archaeology of inland Iberia during the EIA is far less developed, despite being crucial for understanding the whole picture of socio-economic transformations that occurred during this period: it has been proposed that this area witnessed the emergence of centers of political power, which attracted foreign interests (Álvarez-Sanchís, 2000; Ruiz Zapatero and Álvarez-Sanchís, 2015). In this regard, Central Iberia emerges as a paradigmatic region for investigating these matters. Its archaeological record holds abundant and well-preserved settlements and villages, making it a prime location for conducting archaeological research and exploring daily life practices.

Since the 1990s, archaeological excavations and scattered scientific studies in the region have started to shed some light on Central Iberian EIA contexts. Some authors see the beginning of the first millennium BCE in the Northern Iberian Plateau as a time of profound social and economic change (Álvarez-Sanchís et al., 2011; Blanco-González, 2011; Fernández-Posse, 1998) involving demographic growth, a shift in settlement patterns and the consolidation of sedentary lifestyles (Álvarez-Sanchís, 2000; Álvarez Sanchís et al., 2017; Arnaiz Alonso, 2017; Blanco-González and López-Sáez, 2013; Delibes de Castro and Romero Carnicero, 2011). Paleoecological data (Blanco-González and López-Sáez, 2013; López-Sáez et al., 2009) show a transition from Subboreal to Subatlantic climate at the beginning of the 1st millennium BCE, linked to cooler and more humid conditions in the Northern Iberian Plateau. This climatic shift could have triggered economic and social innovations, such as agricultural intensification and sedentism (Delibes de Castro and Romero Carnicero, 2011; Ruiz Zapatero and Álvarez-Sanchís, 2015). In agreement with this hypothesis, the earliest sedentary villages in the region appear around 900 BCE (Álvarez-Sanchís et al., 2011; Álvarez-Sanchís and Ruiz-Zapatero, 2014). These are located at the fertile valleys of the Duero River and its tributaries (Ruiz Zapatero and Álvarez-Sanchís, 2015).

Several hundred EIA villages have been documented to date and they have been the focus of investigations about architectural aspects (Arnaiz Alonso, 2017). These nucleated settlements comprise single-room circular or square earthen houses with adobe walls and clay floors, a clay hearth in the center and one built-in earthen bench placed opposite to the entrance (Delibes de Castro et al., 1995). The diachronic changes identified in these settlements, together with available paleoecological data (Blanco-González and López-Sáez, 2013; López-Sáez et al., 2009), have led to suggest that this massive earthen architecture was linked to increasing sedentism, as well as external influxes, from Southern Iberia and the Mediterranean (Álvarez-Sanchís and Ruiz-Zapatero, 2014; Arnaiz Alonso, 2017).

So far, research has drawn heavily on ethnographic parallels to guess the uses and functions of buildings and areas. However, little is still known about daily life practices and space use within these villages and their dwellings. In fact, a series of shortcomings have hampered further advance in archaeological research at Central Iberian EIA (Álvarez-Sanchís et al., 2011; Esparza Arroyo, 2011): 1) the lack of open-area excavations targeting investigations of intra-site spatial distribution patterns, 2) the inaccuracy of radiocarbon dates –affected by the 'Hallstatt plateau' (*ca.* 800-400 BCE) of the radio-calibrated curve–, and 3) the absence of contextual, stratigraphic and geoarchaeological data, which can provide information about site formation processes, the function, use and evolution of architecture, building technology and living spaces.

The application of archaeological science approaches to EIA central Iberian sites holds great potential for assessing these shortcomings, as well as to explore social, cultural and environmental aspects. Specifically, geoarchaeological approaches through microstratigraphic techniques are essential to provide a wide variety of relevant information about craftsmanship, architecture and domestic life concealed in the sedimentary matrix of dwelling structure infillings, middens, hearths, and earthen architectural elements (Friesem et al., 2017; Gé et al., 1993; Goldberg and Macphail, 2006; Karkanas and Goldberg, 2018; Matthews et al., 1997; Schiffer, 1983; Stoops et al., 2017; Uzdurum et al., 2023). A powerful geoarchaeological tool to investigate such sedimentary artifacts is archaeological soil micromorphology. There is a significant body of micromorphological work on archaeological and ethnoarchaeological household structures from different time periods that provide information about the composition and formation processes of: 1) construction materials and techniques (Cammas, 2018; Cereda and Draganits, 2022; Cereda and Fragnoli, 2021; Cutillas-Victoria et al., 2023; Friesem et al., 2011, 2020, 2017, 2014b; Goodman-Elgar, 2008; Lorenzon, 2021; Lorenzon et al., 2023; Love, 2012; Mateu et al., 2022; Uzdurum et al., 2023) and 2) occupation surfaces and constructed floors (Boivin, 2000; Gutiérrez-Rodríguez et al., 2020; Karkanas and Efstratiou, 2009; Karkanas and Van de Moortel, 2014; Lisá et al., 2020; Lo Russo et al., 2022; Matthews et al., 1997; Milek, 2012; Milek and Roberts, 2013; Nicosia et al., 2022; Shillito and Ryan, 2013; Stahlschmidt et al., 2017).

The application of complementary archaeometric techniques in these contexts, from a microcontextual approach, has provided relevant data towards more accurate interpretations. For instance, inorganic chemistry techniques, such as FTIR, X-Ray fluorescence (XRF) and X-Ray diffraction (XRD), have been useful tools for determining and characterizing floor sequences and construction materials (Anderson et al., 2014; Cereda and Draganits, 2022; Cutillas-Victoria et al., 2023; Lorenzon, 2021; Lorenzon et al., 2023; Milek and Roberts, 2013; Nodarou et al., 2008; Shahack-Gross et al., 2005; Shillito, 2017). Other studies have incorporated phytolith analysis to identify activity areas in different living spaces (Albert et al., 1999, Egüez et al., 2020; Nicosia et al., 2022; Shillito and Ryan, 2013; Sulas and Madella, 2012). Organic geochemistry techniques, including lipid biomarkers and compound-specific stable-isotope analysis, have been so far successfully applied to dump deposits from domestic contexts (Shillito et al., 2011; Shillito and Matthews, 2013), and occupation surfaces (Égüez et al., 2020; Leierer et al., 2019; Tomé et al., 2022), but have not been applied to floors, construction materials and domestic features.

These micro-geoarchaeological approaches have recently been applied to a series of Iron Age settlements from Northeast and South-Eastern Iberia (Belarte et al., 2023; Cutillas-Victoria et al., 2023; Mateu et al., 2013, 2019). From the micromorphological study of earthen material construction fragments from Sant Jaume, Mateu et al. (2013) were able to identify two technical processes that implied the use of earth-based materials: the fabrication of furniture (e.g. boxes, discs), and construction materials belonging to the roof/ceiling and walls of a dwelling. In El Calvari del Molar, Mateu et al. (2019) characterized the semi-cemented living earthen floors within one of the rooms of a dwelling, and identified the materials and techniques that were used during its construction. Belarte et al. (2023) studied clay combustion structures from Masies de Sant Miquel and Tossal de la Vila, recording the earth-based construction materials and techniques that were used, the estimated temperature of burning, and the plants that were selected as fuel. Lastly, in Villares de la Encarnación, Cutillas-Victoria et al. (2023) characterized the mudbricks comprising the site's rampart and identified various potential sources for raw materials used in their crafting. Therefore, there is promising potential in applying these techniques to EIA Central Iberian contexts.

However, the implementation of these high-resolution geoarchaeological techniques can be challenging when applied to archaeological contexts in which earth-based materials and structures represent the main component of the sedimentary deposit, because they tend to become a dense palimpsest of different unidentifiable construction and occupation layers (Bellat et al., 2023; Karkanas, 2019; Mateu et al., 2022). This issue can be especially difficult to solve when the earthen material has suffered decay and collapse processes (Friesem et al., 2014a, 2014b, 2017; Goodman-Elgar, 2008; Karkanas, 2019;

Pastor Quiles, 2017), as it could be easily mistaken as natural, geogenic sedimentary deposits. As a result, identifying occupation layers and/or events becomes a demanding task, and it hampers our chances to accurately study past human behavioral patterns. Consequently, identification and characterization of earth-based materials and construction techniques in these particular sedimentary contexts is crucial for reconstructing past human practices, activities and site use histories.

In this paper, we approach the sedimentary record of Cerro de San Vicente (Salamanca, Spain), a Central Iberian EIA settlement, from a multitechnique, microcontextual geoarchaeological perspective. Our primary research questions cover the following aspects: Firstly, which processes have contributed to the formation of the settlement? Secondly, what were the main construction materials utilized within the site, and how were they used through time? Lastly, is it possible to identify cultural markers through the geoarchaeological study of construction materials and techniques? To address these questions, we applied archaeological soil micromorphology, lipid biomarkers, X-Ray diffraction (XRD) and X-Ray fluorescence (XRF) to undisturbed and loose sediment samples from three different earthen dwelling contexts and construction materials (mudbrick) within Cerro de San Vicente. Our aims are to 1) assess site formation processes and the degree of integrity of the deposit 2) characterize construction materials and techniques, 3) identify the activities carried out in the dwelling structures, and 4) explore dwelling structure histories.

2. Materials and methods

2.1. Cerro de San Vicente: site background

Cerro de San Vicente is an EIA village located in the Northern Iberian Plateau, on the westernmost hill of the current city of Salamanca (Spain) (Fig. 1). It is situated at the top of an Eocene sandstone flat-top hill or mesa at 805 m.a.s.l., on the right bank of the Tormes River. The hill was shaped through the erosive action of the river and its tributaries. The sides of this geomorphological unit are steep, marked by three 30 m-tall, northwest and southeast-facing escarpments above the present-day Tormes River. The eastern slope is perched and faces the La Palma valley, and the northern slope is narrower and easily accessible (Blanco-González et al., 2017). Geologically, Cerro de San Vicente is located on the westernmost edge of the Duero basin, in its contact with the eastern edge of the central Iberian zone of the Hesperian massif (Julivert et al., 1972), which is characterized by discordant siliceous Mesozoic deposits over Paleozoic materials of the variscal substrate.

The prehistoric settlement was discovered in 1951 and has been excavated discontinuously since 1990. Excavations between 2006 and 2022 uncovered a 600 m^2 area at the top of the hill (Fig. 2), focusing on a later occupation phase before the end of the village's biography by the fifth century BCE. Fieldwork in this transect has yielded several earthen dwellings (five roundhouses and two rectangular buildings), thirteen smaller structures of unknown function (presumed to be mud and stone bases of over-ground silos) and open-air transit areas made of compact,

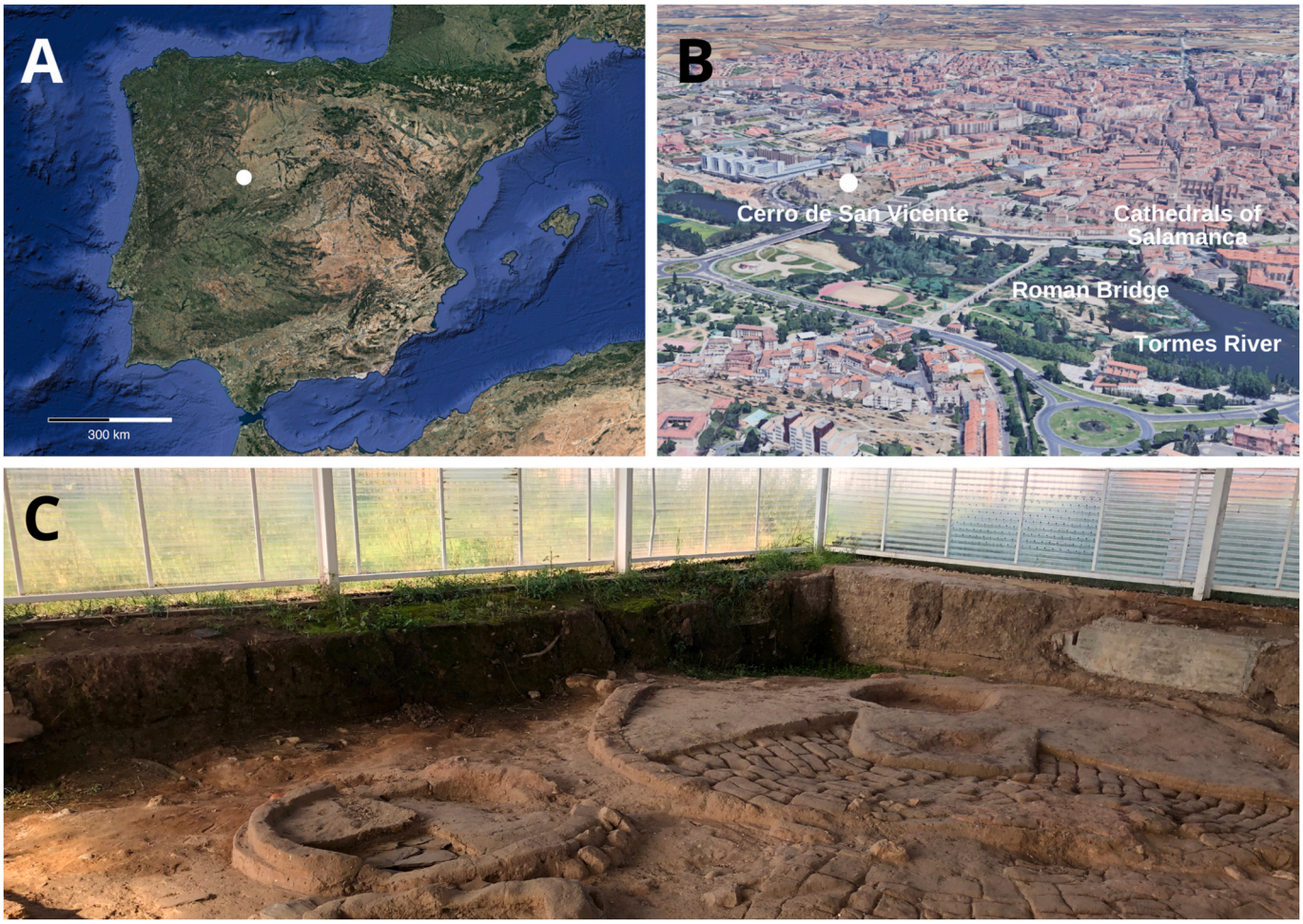

Fig. 1. (A) Geographic location of Cerro de San Vicente in Northern Iberia **(B)** View of the archaeological site and its surroundings **(C)** Partial view of the archaeological site's excavation area, showing two earthen buildings (House 2 and Ancillary Structure). Note the good state of preservation of the dwelling remains, with visible lower parts of the walls, and partially excavated sedimentary fills.

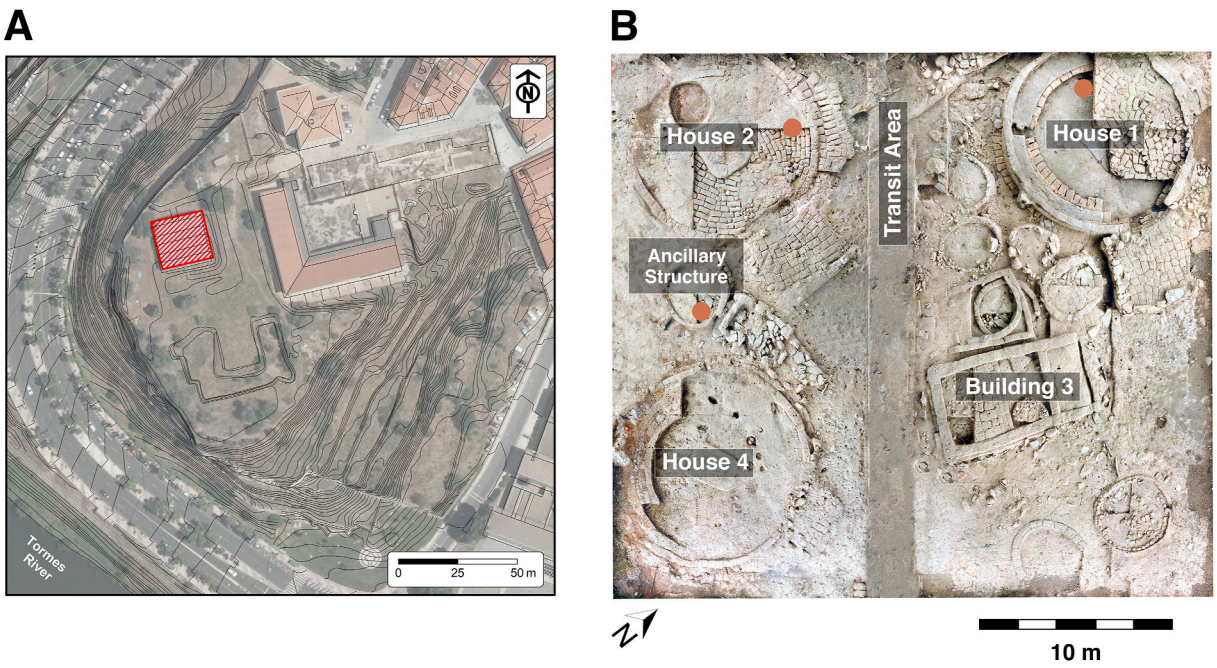

Fig. 2. **(A)** Aerial view of Cerro de San Vicente, with indication of the sector excavated in 2006–2022 (in red) and targeted in this article. **(B)** Plan view of the 400 m^2 sector excavated in 2006–2022, showing earthen dwelling remains. House 1, House 2 and Ancillary Structure have been considered in this study. The orange dots represent the sampled areas (Photogrammetry by A. Martín Esquivel). (For interpretation of the references to color in this figure legend, the reader is referred to the Web version of this article.)

ashy deposits interpreted as middens. The dwellings exhibit a circular floor plan, with walls made with mudbrick, a central clay hearth, one built-in earthen bench and a trapezoidal entrance hall (Blanco-González et al., 2017, 2022; Macarro Alcalde and Alario García, 2021). The cultural rationale of builders drew on the physical superimposition of architectural remains, via the accretion of phases upon phases, leading to a built-up materiality (Blanco-González, 2011; Blanco-González et al., 2022). Very scanty archaeological remains were found inside the documented structures, which might suggest that they were carefully cleaned prior to their final intentional abandonment (Blanco-González et al., 2022, 2023a).

Accurate chronometric data of this last phase of the village was obtained through a combination of radiocarbon, optically stimulated luminescence (OSL) and archaeomagnetic dating (Blanco-González et al., 2022; García-Redondo et al., 2021). These data place one of the main occupations of the site to the late seventh century BCE. The last use of the central clay hearth of one of the roundhouses (House 1) was recently dated by full-vector archaeomagnetism using the SHA. DIF.4 k geomagnetic field model and yielded an age interval between 654 and 575 BCE (with pTRM-check corrected data) (García-Redondo et al., 2021). Stratigraphic data and ceramic refitting suggest that roundhouses and ancillary structures were used roughly at the same time by their inhabitants.

The excavated sector has been very rich in domestic inventories. However, most of the artifacts have been recovered in the ash dump deposits outside the domestic buildings, and therefore they have been interpreted to be refuse in secondary position (Blanco-González et al., 2017, 2022). Archaeological materials consist of abundant hand-made pottery, faunal remains, quern stones, bone and antler utensils related to spinning and weaving, and iron and bronze tools and by-products (e.g., knives, fibulae, slags) (Blanco-González et al., 2017, 2022, 2023a; Macarro Alcalde and Alario García, 2021).

A remarkable collection of Mediterranean imported items has been recovered in the context of House 1: one Egyptian faience bowl, faience beads and amulets, as well as wheel-thrown Egyptian and Phoenician red-slip pottery, including an oil-flask or ampulla for balsam (Blanco-González et al., 2022, 2023a). These findings come together with the identification of on-site performance of extra-regional handicrafts and know-how from faraway Iberian regions (Blanco-González et al., 2023b). House 1 has been interpreted as a paramount roundhouse which likely functioned as a meeting hall, inhabited by the patriarch of an extended household group, hosting banqueting and social activities (Blanco-González et al., 2022, 2023a, 2023b).

2.2. *Archaeological soil micromorphology*

Archaeological soil micromorphology is a branch of geoarchaeology that focuses on the study of undisturbed, oriented archaeological sediment blocks through petrographic microscopic and/or ultramicroscopic techniques. It holds a great potential for the analysis and interpretation of site formation (depositional and postdepositional) processes, sedimentary components, paleoenvironment and microcontextual anthropogenic features (Courty et al., 1989; Nicosia and Stoops, 2017; Stoops, 2003). Recent studies have shown that micromorphology blocks are also a relevant source of contextualized lipid biomarkers (Rodríguez et al., 2020) and ancient DNA (Massilani et al., 2022).

For the analysis, three intact and oriented sediment blocks from House 1, House 2 and its Ancillary Structure (Fig. 3) were collected. Block 1 (House 1) was processed at the Spanish National Research Center for Human Evolution-CENIEH (Burgos, Spain) into two thin sections (14 cm × 6 cm x 30 μm and 9 cm × 6 cm x 30 μm). Blocks 2 (House 2) and 3 (Ancillary Structure) were processed into four thin sections (9 cm × 6 cm x 30 μm) at the Archaeological Micromorphology and Biomarkers Lab (AMBILAB, Universidad de La Laguna, Tenerife, Spain). Two mudbrick samples (see supplementary material) were also transformed into two thin sections at the AMBILAB. The manufacturing procedure in the AMBILAB followed the steps described by Leierer et al. (2020, 2019) and Tomé et al. (2022). First, the blocks are dried for 48 h at 60 °C and impregnated with a 7:3:0.1 v/v/v ratio mixture, made of polyester resin (palatal cast resin UN 1866, TNK compounds), styrene (styrene monomer (CAS: 100-42-5) UN 2055, TNK compounds) and a catalyst (methyl ethyl ketone (Luperox, CAS: 78-93-3), TNK

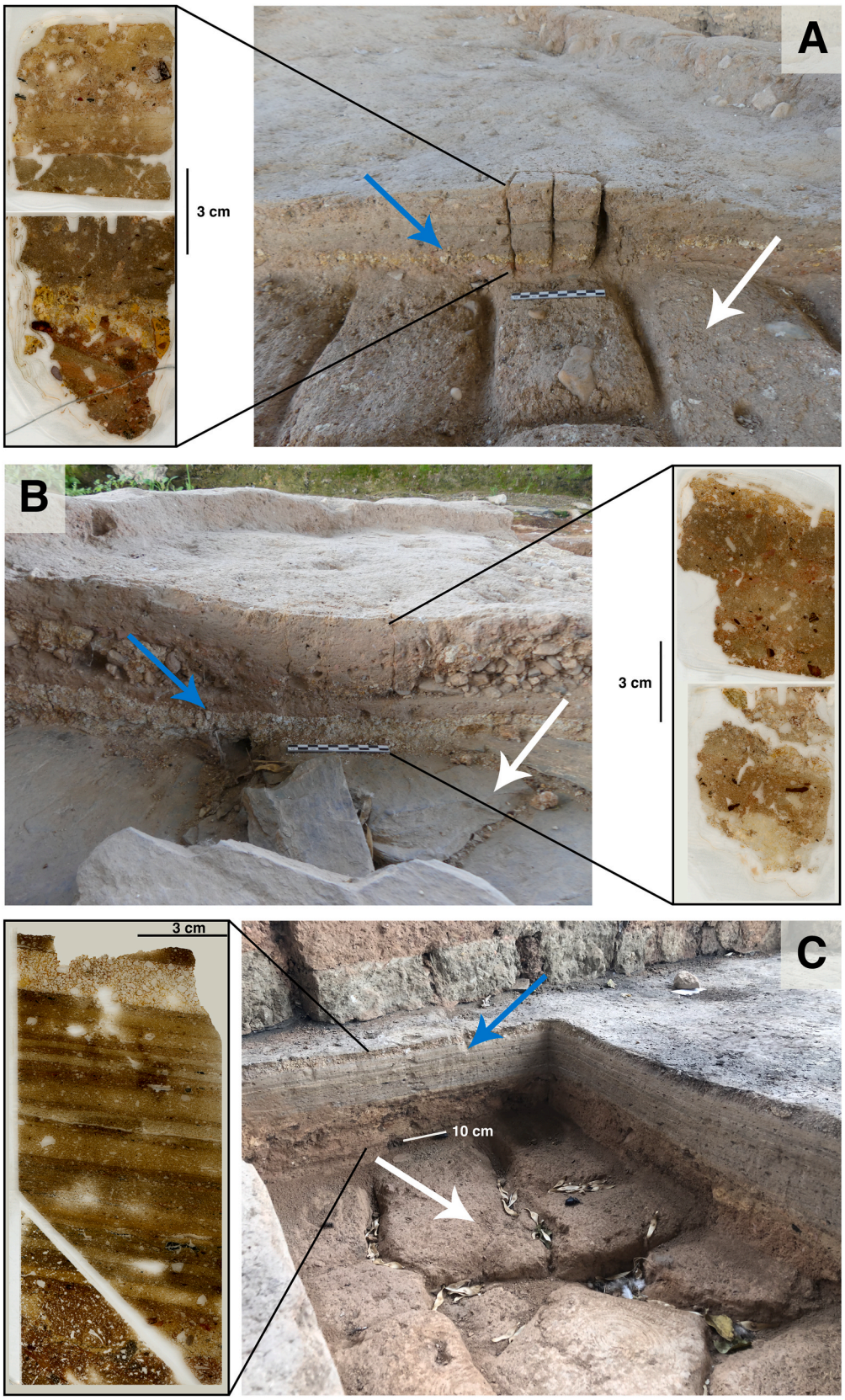

Fig. 3. Photographs and thin section scans of the sampled profiles from each dwelling. **(A)** House 2 **(B)** Ancillary Structure **(C)** House 1. **A** and **B** show a compact yellow rocky layer at the base, overlaid by distinct compact silty-clayey brown layers (blue arrow). The yellow layer in **C** is located at the top of the sequence (House 1's sequence is stratigraphically older) (blue arrow). In House 1 **(C)**, note how the compact silty-clayey brown layers are at the bottom of the yellow rocky layer (blue arrow). Both House 2 **(A)** and House 1 **(C)** exhibit a mudbrick layer at the base (white arrows), whilst the Ancillary Structure's **(B)** base is conformed of slate slabs (white arrow). (For interpretation of the references to color in this figure legend, the reader is referred to the Web version of this article.)

compounds). The consolidated blocks were cut into 1 cm-thick slabs with a radial saw (Euro-Shatal M31100) and glued onto 9 × 6 cm glass slides. Using a precision cutting machine (Uniprec ATA Brilliant-220) their depth was reduced to 1 mm, and then polished down to 30 μm with a grinding machine (G&N MPS-RC-Geology).

The micromorphological analyses were carried out using two petrographic microscopes located in the AMBILAB: Nikon E600-POL and Nikon AZ100 (with epifluorescence module). The Nikon DS-Ri2 and Microvisioneer software (with a Basler acA2400 camera) were respectively used for taking microphotos and for performing high resolution thin section scanning. The thin sections were observed in plain polarized (PPL) and cross polarized light (XPL).

The standard guidelines provided by Stoops (2003) and Nicosia and Stoops (2017) were followed for thin section description. In addition, we have used the concept of Microfacies Unit (MFU) applied to archaeological soil micromorphology, and the Microfacies Types (MFT) approach to group microfacies units with similar micromorphological characteristics (Courty, 2001; Fernández-Palacios et al., 2023; Karkanas et al., 2015; Lisá et al., 2020; Tomé et al., 2022; Villagran et al., 2009). This approach aims to facilitate our understanding and interpretation of site formation processes through the determination of specific combinations of micromorphological features (Goldberg et al., 2009).

2.3. Lipid biomarkers

2.3.1. Lipid extraction, analysis, and quantification

For this study, 22 bulk sediment samples were collected from three different floor sequences, with the aim of collecting one sample per visible sedimentary facies and/or layer. In House 1 (where micromorphology Block 1 was extracted), 8 samples were obtained directly from the targeted stratigraphic sequence. For House 2 and the Ancillary Structure (micromorphology blocks 2 and 3), two sub-blocks were collected, and were later excavated and subsampled into 5 and 9 bulk sediment samples in the AMBILAB. Two bulk sediment samples were also acquired from two mudbricks from the site. All the samples were taken using sterilized metal tools and nitrile gloves, packed in aluminum foil to avoid phthalate contamination, and finally stored at −20 °C.

All the samples were analyzed at the AMBILAB, following the procedure described by Connolly et al. (2019), Jambrina-Enríquez et al. (2018), Leierer et al. (2019) and Tomé et al. (2022). First, 5 g of homogenized sediment were collected for each sample to extract their Total Lipid Extract (TLE). Using an ultrasound-assisted solid-liquid extraction method, lipids were extracted employing a 40 mL 9:1 v/v mixture of dichloromethane (DCM)/methanol (MeOH) under ultrasonic irradiation for 30 min (USC 600th from VWR International, Barcelona, Spain). Then, the mixture was centrifuged at 4700 rpm/10 min (Mega Star 1.6 from VWT International) and filtered through pyrolyzed glass wool. This procedure was repeated three times. Finally, the TLE was evaporated under Nitrogen flow at 40 °C (RapidVap® Vertex Evaporator from Labconco, Missouri, USA). The TLE was then fractionated into 6 different lipid groups or fractions (*n*-alkanes, aromatics, ketones, alcohols, fatty acids and other compounds) (**Table 1**) using a chromatographic column, made of 1 g of calcined silica gel (70–230 mesh) and 0.1 g of sterilized sand (50–70 mesh). Each lipid fraction was evaporated under Nitrogen flow and stored at −20 °C until the analysis. The internal standard (IS) was also added to each fraction (**Table 1**).

Table 1
Solvents, elution volumes and internal standards used in the extraction of the different lipid fractions.

Fraction	Solvents and elution	Internal Standard (IS)
1 *n*-alkanes	3/8 dead volume (DV) *n*-Hexane	5α-androstane
2 aromatics	2 DV 8:2 v/v *n*-Hexane/DCM	Acenaphthene
3 ketones	2 DV DCM	5α-androstane
4 alcohols	2 DV 1:1 v/v DCM:EtOAc	5α-androstan-3β-ol
5 fatty acids	2 DV EtOAc	Methyl C19:0
6 other compounds	2 DV MeOH	Methyl C19:0

Alcohols and fatty acids were derivatized to obtain trimethylsilyl esters (TMS) and methyl-esters, respectively. For the alcohols, 100 μL of N, O-Bis (trimethylsilyl) trifluoroacetamide (BSTFA) and trimethylchlorosilane (TCMS) 99:1 v/v were added, and then the mixture was derivatized at 80 °C for 1 h. After drying, it was reconstituted with 50 μL of DCM. Fatty acids were derivatized by adding 5 mL of MeOH and 400 μL of H_2SO_4 to each sample. The mixture was heated at 70 °C for 4 h, and then neutralized with a sodium bicarbonate saturated solution. Methyl-esters were extracted three times employing 3 mL of *n*-hexane, then dried under Nitrogen flow and reconstituted with 50 μL of DCM per sample.

Measuring was carried out using gas chromatography (GC) after the reconstitution of each fraction using solvent (DCM). An Agilent 7890 B gas chromatograph was used to determine and quantify the compounds present in the sediment. It is attached to a 5977 A single quadrupole (Q) MSD with an electron impact interface, equipped with an automatic autosampler and a multimode injector (Agilent Technologies, Waldbronn, Germany). To control the system, acquire and process the data, The MassHunter Workstation Software was employed.

The equipment conditions for *n*-alkanes were similar to the ones described by Herrera-Herrera et al. (2020), and for aromatics, ketones, alcohols, fatty acids and other compounds, as shown by Herrera-Herrera and Mallol (2018), Jambrina-Enríquez et al. (2018) and Tomé et al. (2022) (a detailed description is presented in supplementary material). After detection and measuring, the compounds were identified by comparing their retention times and reference spectra and using NIST Mass Spectrum Library. *n*-Alkanes were quantified with calibration curves (obtained by plotting the Area/AreaIS ratio against the concentration of reference standards), after taking the four most intense fragment ions (m/z 43, 57, 71, 85 for alkanes; m/z 67, 81, 95 and 245 for the IS). For the other fractions, the concentrations were estimated through comparison with the IS area. Concentrations are presented in μg per gram of dried sample (μg/gds) (*n*-alkanes) and ng per gram of dried sample (ng/gds) (other fractions).

In order to ease the *n*-alkane data interpretation, two indexes were calculated employing the quantifications obtained from the calibration curves: **a)** OEP (nC_{27}-nC_{33}) (odd-over-even predominance), to determine the conservation degree of organic matter (Hoefs et al., 2002) and **b)** ACL (nC_{25}-nC_{33}) (average chain length), to evaluate the main features of the biomass (Freeman and Pancost, 2014) (see supplementary material).

2.4. Mineralogical (XRD) and elemental geochemical (XRF) analyses

Mineralogical composition of the sediments was semiquantitatively (% weight) analyzed in the I+D+i Scientific-Technological Center of Universidad de Burgos (Spain). Samples were carefully dry-cleaned and powdered using an agate mortar. The semiquantitative mineralogical analysis was performed in a Bruker D8 Advance diffractometer, and the *DIFFRACplus basic EVA* software was used for diffractogram interpretation and mineral identification. The limit of detection used in the analysis was stablished at 1% wt.

The semiquantitative elemental geochemical analysis (% weight) of the samples was performed through X-ray Fluorescence (XRF). The sediment samples were powdered, homogenized, mixed with flux (Lithium Metaborate/Tetraborate, 0.5% KBr) and transformed into beads using an Equilab F1 Induction fluxer. The analysis of the beads was carried out at the Scientific and Technological Park of the University of Burgos, using a Thermo ARL ADVAT XP Sequential XRF spectrometer. The limit of detection of the XRF equipment is 0.01% wt, but we only considered the data obtained for major elements well above 1% wt. The WinXRF.ADVANT 3.2.1 and UNIQUANT v.5.47 software packages were used for data interpretation.

3. Results

3.1. Archaeological soil micromorphology

3.1.1. Lithology, microstructure, porosity and main components

The three sequences showed a homogeneous lithological composition, mainly consisting of terrigenous, siliciclastic sediments with angular and subangular quartz grains, oscillating between silt and gravel. Gravel and sand-sized angular and subangular slate, as well as silt-sized mica-group minerals were also recurrently identified.

Two types of microstructure were identified throughout the sequences: 1) a massive microstructure, prevailing in most of the microfacies, and 2) a complex microstructure, composed of massive and intergrain microaggregate patches. The samples predominantly showed random, close space porphyric c/f related distribution. Vughs are the most abundant porosity type. Planes, moldic voids, vesicles and channels were also identified.

Anthropogenic and biogenic components are scarce, mainly consisting of unidentified, silt-sized charred plant material, charcoal, mineral temper aggregates, calcitic ash, disorthic and anorthic clay nodules and earth-based construction material fragments (Table 2, Fig. 4).

3.1.2. Microfacies units (MFU) and microfacies types (MFT)

According to the features shown in 3.1.1 we have identified 30 microfacies units in House 1, 13 in House 2, 6 in the Ancillary Structure and 1 in each mudbrick sample. These microfacies are associated with 24 biomarker samples (Fig. 5 and supplementary material). In order to facilitate the interpretation of the sequences, these microfacies units have been grouped into 5 microfacies types (MFT) (Table 3, Fig. 6, supplementary material).

3.2. Lipid biomarkers

3.2.1. n-Alkanes

n-Alkane data was obtained for the 24 bulk sediment samples (Fig. 7). In House 1's sequence, the *n*-alkane distribution ranges from nC_{20} to nC_{33}, with concentrations between 0.10 and 0.04 μg/gds. For House 2, the distribution varies from nC_{18} to nC_{37}, and the *n*-alkane concentration from 0.10 to 0.07 μg/gds. Finally, the Ancillary Structure showed a nC_{17} to nC_{37} *n*-alkane distribution, with concentrations ranging from 0.16 to 0.07 μg/gds. Mudbrick samples presented a nC_{20} to nC_{35} *n*-alkane distribution, and concentrations of 0.08 and 0.06 μg/gds.

n-Alkane indexes (OEP and ACL) were calculated for all the samples (see supplementary material). In House 1, OEP values oscillate between 3.66 and 2.02, and ACL between 30.07 and 29.47. For House 2, OEP ranged between 2.92 and 1.63, and ACL between 29.59 and 28.18. The Ancillary Structure's sequence showed OEP values which fluctuate between 5.33 and 1.32, while ACL ranges between 29.19 and 28.52. Lastly, mudbrick samples presented OEP values between 1.82 and 1.36, and ACL between 29.23 and 28.96.

3.2.2. Other compounds

Ketones, alcohols and acids were identified, and their concentration was estimated in the 24 bulk sediment samples. Among the different compounds, there is a significant recurrence of, cholesterol and other sterols, lactones, short to mid-chain alcohols and fatty acids, as well as oleic and abietane-type acids (abietic, dehydroabietic and 7-oxodehydroabietic acid) throughout the three sequences. Mudbrick samples only showed palmitic and stearic acid. A detailed list of the identified compounds and their estimated concentration is presented in supplementary material.

3.3. Mineralogical (XRD) and elemental geochemical (XRF) analyses

XRD analysis showed a homogeneous mineralogical composition for all the sediment samples, mainly consisting of quartz, feldspars (albite and orthoclase) and clay minerals (kaolinite and muscovite). On the other hand, the elemental geochemical composition analysis (XRF) also yielded a uniform distribution for all the samples, with SiO_2 as the predominant compound (between 79% and 69%), followed by Al_2O_3 (from 17% to 12%) and Fe_2O_3 (between 7% and 3%). The presence of CaO, K_2O, Na_2O, MgO, and TiO_2 was also documented, but in lower proportions (less than 3%). A detailed description of the mineralogical and elemental geochemical composition of the samples is provided in supplementary material.

Table 2
Description of the main components identified in the micromorphological samples. Microphotographs of each component are presented in Fig. 4.

Component	Description	Significance
Charcoal	Present in House 1 and House 2 Abundant in House 1, especially at the bottom of the sequence Rounded and angular, sand-sized	Wood burning activity
Charred plant material	Present in House 1, House 2, and Ancillary Structure Abundant in House 1 and House 2 Rounded, silt and sand-sized Unidentified	Plant burning activity. Suggests low burning temperatures
Calcitic ash	Present in House 1, House 2, and Ancillary Structure More abundant in House 1 Displayed in thin patches, reworked Calcium oxalate pseudomorphs Usually mixed with unidentified, silt-sized charred plant particles and charcoal fragments	Wood burning activity. Implies high burning temperatures
Clay nodules	Present in House 2, Ancillary Structure and Mudbrick 2 More abundant in Ancillary Structure Disorthic and anorthic Typic, inequigranular nodules Size ranges between 800 and 400 μm Mainly composed of dark brown clayey micromass, undifferentiated	Suggests use of water in the crafting of earth-based materials
Mineral grains	Very few, present in House 2 and Ancillary Structure Angular and subrounded Ferruginous	Suggests the use of mineral temper for earth-based construction
Earth-based construction materials	Present in House 1, House 2, Ancillary Structure, Mudbrick 1 and Mudbrick 2 Abundant Dark/light brown clayey micromass, undifferentiated Horizontal particle orientation, random c/f related distribution, compact Vughs, planes, moldic and elongated voids Angular and subrounded Variable preservation states, from degraded to intact Mudbrick and earthen floor fragments, which exhibit the main features described in Table 3 (Microfacies Type 2 and 5)	Suggests mixing of different earth-based construction materials and/or decay and collapse of earth-based construction materials

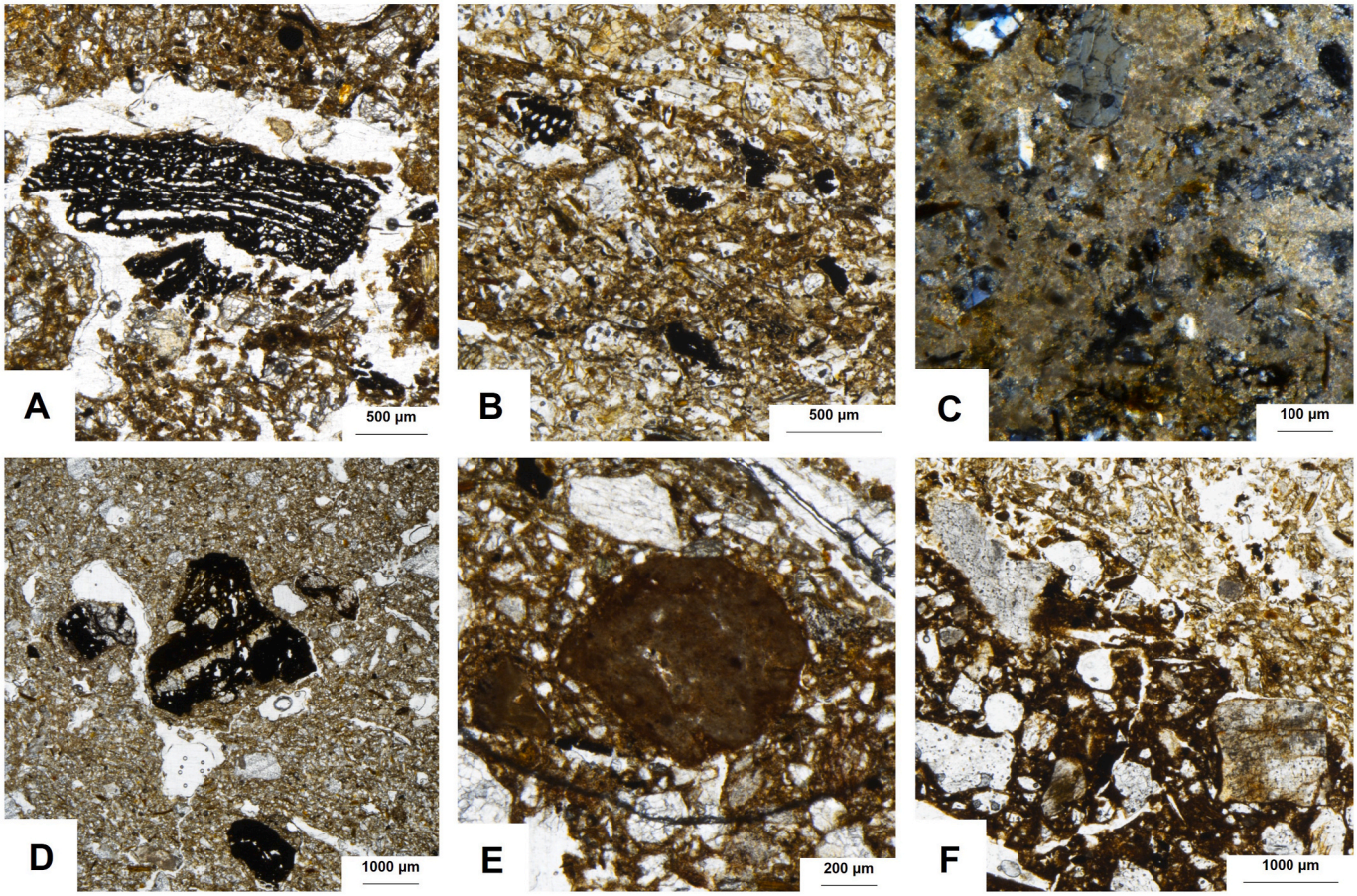

Fig. 4. Microphotographs of the most representative microscopic components identified in the sedimentary sequences. Overall, scarce coarse fraction (submillimetric to subcentimetric) has been documented, and it is usually presented isolated and randomly arranged. A more detailed description of each component is presented in Table 2. **(A)** PPL. Charcoal. It is abundant in House 1, and it is presented in an angular and rounded shape. **(B)** PPL. Unidentified silt-sized charred plant matter. Abundant in House 1 and House 2. **(C)** XPL. Calcitic ash. Usually reworked, mixed with clay, charcoal, and earth-based construction materials. **(D)** PPL. Mineral grains. Ferruginous and subrounded, identified in House 2 and Ancillary Structure. **(E)** PPL. Anorthic clay nodule. Usually composed of undifferentiated clay. Present in House 2, Ancillary Structure and mudbricks. **(F)** PPL. Earth-based construction material fragment (mudbrick). Present in House 1, House 2 and Ancillary Structure. Typically well-preserved, with sharp and defined boundaries and elongated and moldic voids.

4. Discussion

The primary goal of this study is to assess site formation processes, with the aim of identifying and characterizing 1) construction materials and techniques, and 2) activity/occupation layers within the selected dwelling structures. Our micromorphological, mineralogical and molecular data have led us to isolate and characterize multiple construction layers (MFT 1, 2 and 3a), periods of abandonment and decay of the constructive earth-based material (MFT 3 b), and occupation/activity layers (MFT 4). We have also characterized undisturbed mudbricks (MFT 5), one of the most abundant construction materials in the site. Our high-resolution lipid biomarker sampling has allowed us to document the preservation in significant concentrations of lipid biomarkers in all the sequences (*n*-alkanes, ketones, alcohols and fatty acids), associated with construction and activity layers. In the following sections, we discuss the results, and propose possible interpretations and archaeological implications.

4.1. Construction materials and techniques

Micromorphological, mineralogical, and lipid analyses have enabled the identification of three types of construction layers (MFT 1, 2, and 3) that have been consistently observed across all sequences (see Table 3, supplementary material). On the one hand, MFT 1 comprises compact deposits consisting of a homogeneous light-yellow clayey groundmass mixed with sand-sized quartz grains of variable size. The micromorphological features of these layers, such as the horizontal orientation of particles, uniformity of the groundmass, presence of desiccation features, and low occurrence of voids, primarily vughs and vesicles, indicate that these layers have been artificially constructed. The artificial crafting process likely involved the use of moderate to low amounts of water (Bellat et al., 2023; Cammas, 2018; Friesem et al., 2017). Based on the classification proposed by Bellat et al. (2023), these layers can be considered moderately prepared. Based on their prominent micromorphological features (Fig. 8) and their consistent stratigraphic position (always found beneath MFT 2 layers with sharp contacts), MFT 1 can be interpreted as floor preparation layers (Bellat et al., 2023; Gé et al., 1993; Mateu et al., 2019; Matthews et al., 1997). MFT 2 comprises homogeneous, compact deposits consisting of a well-mixed brown clayey groundmass. The presence of clay linings and coatings (Fig. 8), and abundant vughs and vesicles indicates the use of high amounts of water during their preparation (Cammas, 2018; Friesem et al., 2011, 2017; Matthews et al., 1997). The homogeneity of the groundmass and the horizontal orientation of coarse fraction components suggest careful mixing and deposition through direct shaping or kneading techniques (Friesem et al., 2017; Mateu et al., 2019; Pastor Quiles, 2017; Pastor Quiles et al., 2019). These features strongly suggest that MFT 2 represents clay floors (Cammas, 2018; Friesem et al., 2017; Lisá et al., 2020; Macphail and Goldberg, 2018; Mateu et al., 2019). In the case of House 1, these floors appear to have been "mud plastered" (Macphail and

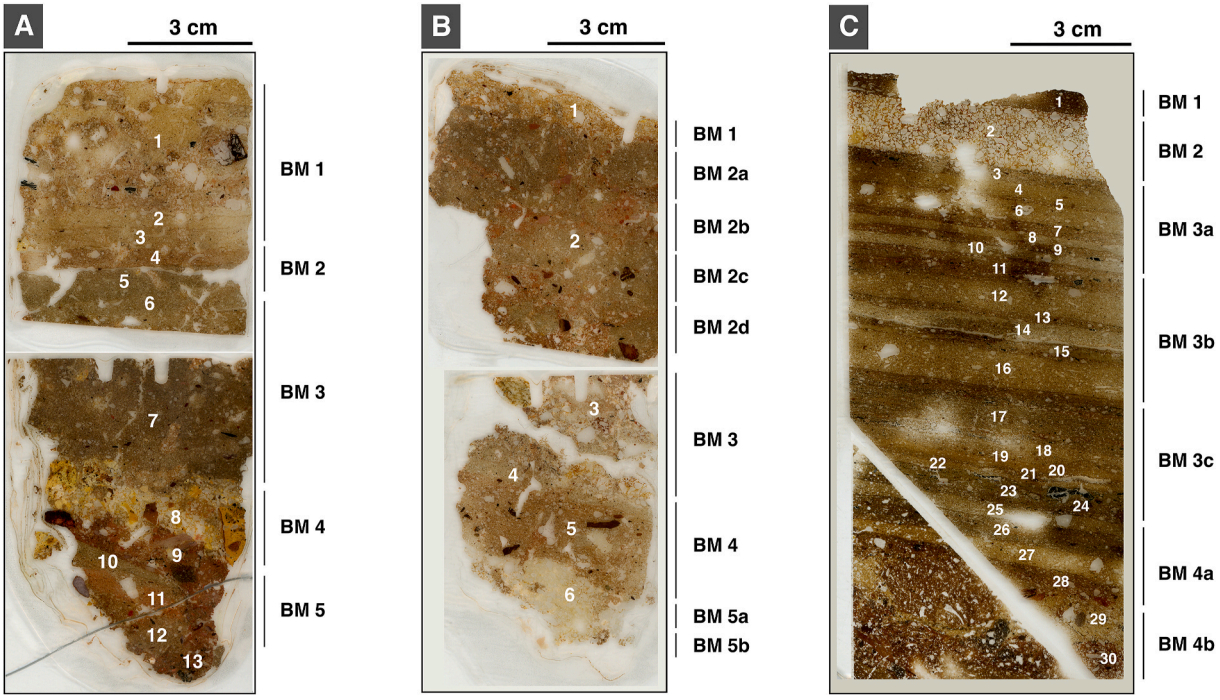

Fig. 5. Thin section scans of each sequence, including microfacies units (MFU) and associated biomarker samples (BM). **(A)** House 2 **(B)** Ancillary Structure **(C)** House 1.

Goldberg, 2010), as evidenced by clear clay linings in the upper contact (Fig. 8). Lastly, MFT 3 exhibits significant differences between MFT 3a and MFT 3b. MFT 3a consists of a heterogeneous, randomly distributed, compact mixture of brown/reddish clay, anorthic and disorthic clay nodules, and other earthen material aggregates. Based on these micromorphological features, MFT 3a can be interpreted as floor preparation layers (Belarte et al., 2023; Bellat et al., 2023; Gé et al., 1993; Mateu et al., 2019; Matthews et al., 1997) that were poorly crafted (Bellat et al., 2023; Cammas, 2018; Courty et al., 1989; Macphail and Goldberg, 2010). In contrast, MFT 3 b also consists of heterogeneous, compact deposits with similar components as MFT 3a but exhibits recurrent pedofeatures associated with bioturbation and postdepositional/decay phenomena (e.g., channels, chambers, calcium carbonate hypocoatings around voids). Therefore, MFT 3b likely represents instances of abandonment and decay of earth-based construction materials.

Lipid biomarkers have been identified in association with all layers within the dwellings (MFT 1, MFT 2, MFT 3, MFT 4) as well as in undisturbed mudbrick samples (MFT 5). The presence of medium to odd long-chain *n*-alkanes (ranging from nC_{17} to nC_{37}), along with OEP and ACL values and the abundance of fatty acids and alcohols, indicates excellent preservation of lipids at the site. However, it is crucial to ascertain the primary source of these sedimentary lipids to facilitate further archaeological interpretations. In this case, a minimum of three potential sources of lipids (either individually or in combination) should be considered: 1) the clayey groundmass used in construction and/or its surrounding vegetation (i.e., natural vegetation in the areas where raw materials were obtained), 2) construction materials and techniques (such as the use of plant-based temper or other plant/animal by-products in the floor crafting process), and/or 3) organic residues resulting from activities carried out by the ancient inhabitants inside the dwellings.

Our data can provide insights into this issue. Firstly, XRD and XRF analyses reveal a homogeneous mineralogical composition in all samples, indicating that the raw material used for floor construction was likely consistent. Micromorphological analysis also indicates minimal differences in the composition of the groundmass within the floors. These differences primarily involve the abundance, type, and particle size of quartz grains and other lithological components (such as slate and mica-group minerals), as well as subtle color variations in the matrix. Moreover, microscopic observations suggest that the use of plant temper as a construction material was limited, since elongated and moldic voids, which are indicative of such temper, are not prominently present. Examination of undisturbed mudbrick samples from the site (MFT 5) displayed similar micromorphological features to those documented in the floors (see Fig. 8, supplementary **material**, Table 3). Therefore, if the construction material or added temper/aggregates were the main sources of lipids, minimal differences in the lipid content across all biomarker samples would be expected. However, the mudbrick control samples yielded only low concentrations (ranging from 0.06 to 0.08 μg/gds) of *n*-alkanes (ranging from nC_{20} to nC_{35}) (Fig. 7), along with palmitic and stearic acids. When comparing the lipid profiles of mudbricks to the biomarker samples from House 1, House 2, and the Ancillary Structure, several distinctions become apparent. The biomarker samples from the houses and Ancillary Structure exhibit higher concentrations of *n*-alkanes, particularly longer-chain *n*-alkanes, and a wider variety of fatty acids, ketones, alcohols and terpenoids (see supplementary material, Fig. 7).

These results suggest that a portion of the lipid biomarkers documented in the sediments could likely originate from the construction material itself (such as the clayey groundmass and/or its supply area) or other added temper/aggregates, as we have observed similar lipids in our control mudbrick samples and sediment samples from the floors. However, we suggest that a significant portion of the lipids identified within House 1, House 2, and the Ancillary Structure can be attributed to human occupation and domestic use of the dwellings. These lipids exhibit a diverse and rich profile that varies across different floor layers. This suggests that the lipid composition of the floors can serve as a valuable tool for examining aspects of human behavior, spatial utilization, and daily life practices. Further details on this topic will be provided in the following section.

Nevertheless, it is important to note that while we can link the biomarker samples to different groups of microfacies units within each dwelling (as shown in Fig. 5), we cannot establish precise connections between the lipid content and specific microfacies and their associated

Table 3
Microfacies types (MFT) identified in the micromorphological samples and their correlation with Microfacies Units (MFU). Microphotographs of each MFT are presented in Fig. 6.

Microfacies Type	Description	Layer Type	Microfacies Unit
1	Deposit made of homogeneous, light-yellow silty-sandy clay and sand-sized quartz grains.	Construction layer	
	1a: Fine quartz sand with 10–15% light-yellow silty-sandy clay. Thin, horizontally layered deposits (around or less than 1 cm).		**House 1**: 10, 12 14, 18, 22 **House 2**: 6, 10 **Ancillary Structure**: 4
	1b: Coarse quartz sand and 30–35% light-yellow silty-sandy clay, with iron staining. Thick deposits (ranging between 2 and 3 cm) with random c/f related distribution.		**House 1**: 2 **House 2**: 8 **Ancillary Structure**: 6
2	Compact deposit composed of homogeneous, massive brown silty-sandy clayey groundmass (60–65%) with sand-sized quartz inclusions. Vughs are the most common porosity type. Moldic voids, horizontal layering and clay linings are also recurrent features.	Construction layer	
	2a: Dark brown, homogeneous silty-sandy clayey groundmass with sand-sized quartz and slate inclusions. Abundant vughs, moldic voids and clay coatings. Compact and massive. Thickness ranges between 2 and less than 1 cm.		**House 1**: 1, 3, 7, 9, 11, 13, 15, 19, 21, 24, 26, 28 **House 2**: 11 **Ancillary Structure**: 5
	2b: Massive deposits of light brown silty-sandy clayey groundmass, with sand-sized quartz and slate inclusions. Abundant planes and other desiccation features. Vughy porosity. Thickness ranges between 5 and around 1 cm.		**House 1**: 4 6, 8.16, 20.25.27 **House 2**: 3, 4, 5, 7
3	Compact and massive deposit, composed of heterogeneous silty-sandy clayey groundmass with orthic and disorthic clay nodules. Thick deposit, raging between 5 and 2 cm.		
	3a: Heterogeneous silty-sandy clayey groundmass (25–30%), with abundant orthic and disorthic clay nodules. Compact, massive, and mostly well-preserved. Recurrent components are earth-based construction material and mineral temper fragments.	Construction layer	**House 1**: 29, 30 **House 2**: 9, 12, 13 **Ancillary Structure**: 3
	3b: Thick, disturbed deposits composed of heterogeneous light brown silty-sandy clayey groundmass (40–50%) with abundant orthic and disorthic clay nodules. Channels, chambers, and planes are the most abundant porosity type, usually presented with strongly developed calcium carbonate coatings.	Decayed construction layer	**House 2**: 1, 2 **Ancillary Structure**: 1, 2
4	Deposit composed of reworked calcitic ash patches and charcoal fragments and compact silty-sandy clays. Main components include charcoal, unidentified silt-sized charred plant material and calcitic ash.	Activity layer	**House 1**: 11, 15, 17, 21, 23, 24
5	Compact light yellow silty-sandy clayey groundmass (20–25%), with abundant sand-sized quartz and slate grains. Abundant vughs and moldic voids. Poorly developed clay coatings.	Mudbrick	**Mudbrick 1** **Mudbrick 2**

MFTs. Although we conducted high-resolution sampling for lipid biomarker analysis, we were unable to isolate the different microfacies units in most cases. Future studies conducted at Cerro de San Vicente (and other sites with similar sedimentary contexts) should consider implementing more precise sampling techniques, such as microdrilling of micromorphology blocks (Rodríguez et al., 2020). This approach would allow us to determine if the lipid content is solely present in the floor layers (MFT 2) or if it is also found in floor preparation layers (MFT 1, MFT 3a). Consequently, we would ascertain if significant differences in lipids exist that could be linked to human activities and/or spatial utilization.

4.2. *Use of space and daily life practices*

Based on micromorphological, mineralogical, and lipid biomarker analyses, we have differentiated and characterized three distinct types of construction layers within the site. These layers include clay floors (MFT 2), floor preparation layers (MFT 1, MFT 3a), and phases of abandonment and decay of earthen construction material (MFT 3b). These construction layers are consistently observed in the three dwelling sequences, exhibiting similar building patterns (Fig. 9).

In House 1 and House 2, MFT 3a is placed at the lowest section of the sequence, likely used for ground leveling before the construction of the floors (Bellat et al., 2023; Gé et al., 1993; Macphail and Goldberg, 2010; Mateu et al., 2019). These preparation layers are followed by meticulously crafted clay floors (MFT 2). In all three dwelling sequences, but particularly in House 1, these clay floors are repeatedly constructed over time, typically preceded by MFT 1 as another preparation layer for the new floor. These events of floor construction can be interpreted as maintenance practices aimed at renovating, preserving and/or refurbishing the interior of the dwellings (Boivin, 2000; Karkanas and Efstratiou, 2009; Lisá et al., 2020). Furthermore, we have observed instances of floor renewal while they were still in use, as indicated by the presence of reactive layers formed by trampling (Gé et al., 1993) which are subsequently replastered. In House 1, we have also identified MFT 4, thin deposits consisting of a mixture of clay, earth-based construction materials, calcitic ash, charcoal, and unidentified silt-sized plant charred particles. We propose that MFT 4 represents active zones/layers (Gé et al., 1993; Macphail and Goldberg, 2010) deposited on top of clay floors (MFT 2), and therefore serve as a potential source of data for understanding space utilization and daily life practices within the dwellings. However, these active layers are not abundant in House 1 and have not been identified in House 2 or the Ancillary Structure. This suggests that the floors were either regularly swept and cleaned and/or covered with blankets made from plant fibers, actively maintained while in use. Although we have not identified any *in situ* mats or carpets (which could be evidenced by the presence of an *in situ* phytolith layer, for instance), the general absence of anthropogenic material fillings in the upper contacts of the floors (which is a recurring effect of trampling on constructed floors) (Gé et al., 1993; Macphail and Goldberg, 2010; Rentzel et al., 2017) and the excellent preservation of millimeter-to-centimeter-thick clay floors could support the hypothesis of the use of mats. The cycles of renewal and maintenance of the dwellings came to an end when an abandonment phase took place around 550 BCE (Blanco-González et al., 2022). Micromorphologically, we have identified deposits resulting from the abandonment and decay of the earthen construction material (MFT 3 b), which are evident in the upper segments of the sequences in House 2 and the Ancillary Structure (Fig. 9). However, these abandonment events do not correlate with the terminal phase of the village (*ca.* 400 BCE), which is not preserved in this excavated sector due to truncation of the uppermost stratigraphy.

Micromorphological observations have provided insights into the functionality of these earthen buildings. In House 1, the analysis of MFT 4 has enabled the identification of various indicators of past human activities. These indicators include combustion residues such as charcoal, silt-sized charred plant material, and reworked calcitic ash. These

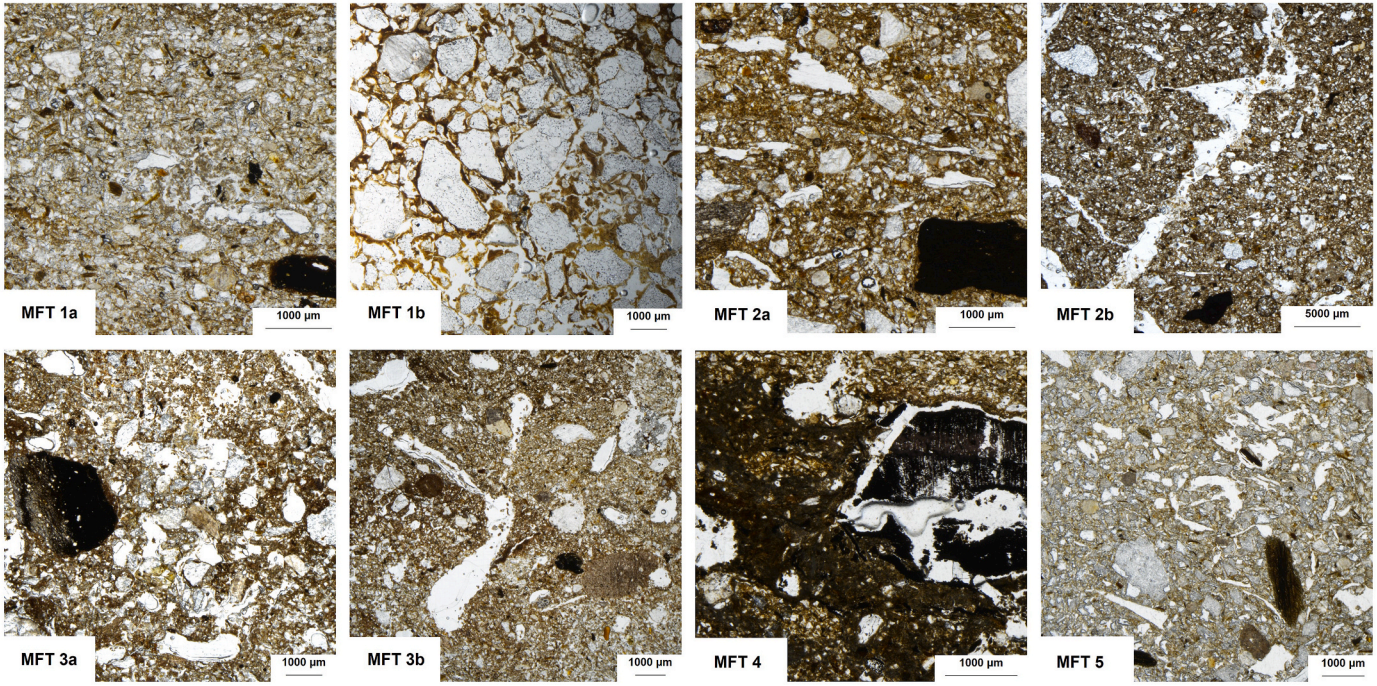

Fig. 6. Microphotographs (PPL) of each Microfacies Type (MFT) identified in the micromorphological samples. A detailed description of each type is presented in Table 3. **MFT 1a)** Constructed floor composed of fine quartz sand and homogeneous, light-yellow silty-sandy clay matrix. **MFT 1b)** Constructed floor. Chitonic, gefuric coarse quartz sand and light-yellow clayey micromass, with clay coatings. Note the iron staining on the top half, where the clay matrix is darker and reddish. **MFT 2a)** Constructed floor composed of massive, homogeneous silty-sandy clay matrix with abundant vughs and diffuse elongated voids forming parallel horizontal bedding. **MFT 2b)** Constructed floor. Massive deposit of light silty-sandy clayey groundmass, with vughy porosity and abundant desiccation features. **MFT 3a)** Constructed floor. Massive, compact heterogeneous silty-sandy clay deposit, with moldic and vugh porosity, abundant disorthic clay nodules, slate fragments and coarse quartz sand. **MFT 3b)** Decayed earth-based construction materials. Compact heterogeneous silty-sandy clay with rounded and subrounded clay nodules, and abundant coarse quartz sand and slate fragments. Channeled microfacies with post-depositional iron staining and hypocoatings (note the darker matrix in the top of the slide, as well as forming rings around the pores). **MFT 4)** Activity layer. Compact silty-sandy clays with frequent charcoal fragments, reworked calcitic ash and sharp disorthic nodules. **MFT 5)** Mudbrick. Compact, homogeneous silty-sandy clayey groundmass, with moldic porosity and detrital rock fragments (coarse quartz sand and slate). (For interpretation of the references to color in this figure legend, the reader is referred to the Web version of this article.)

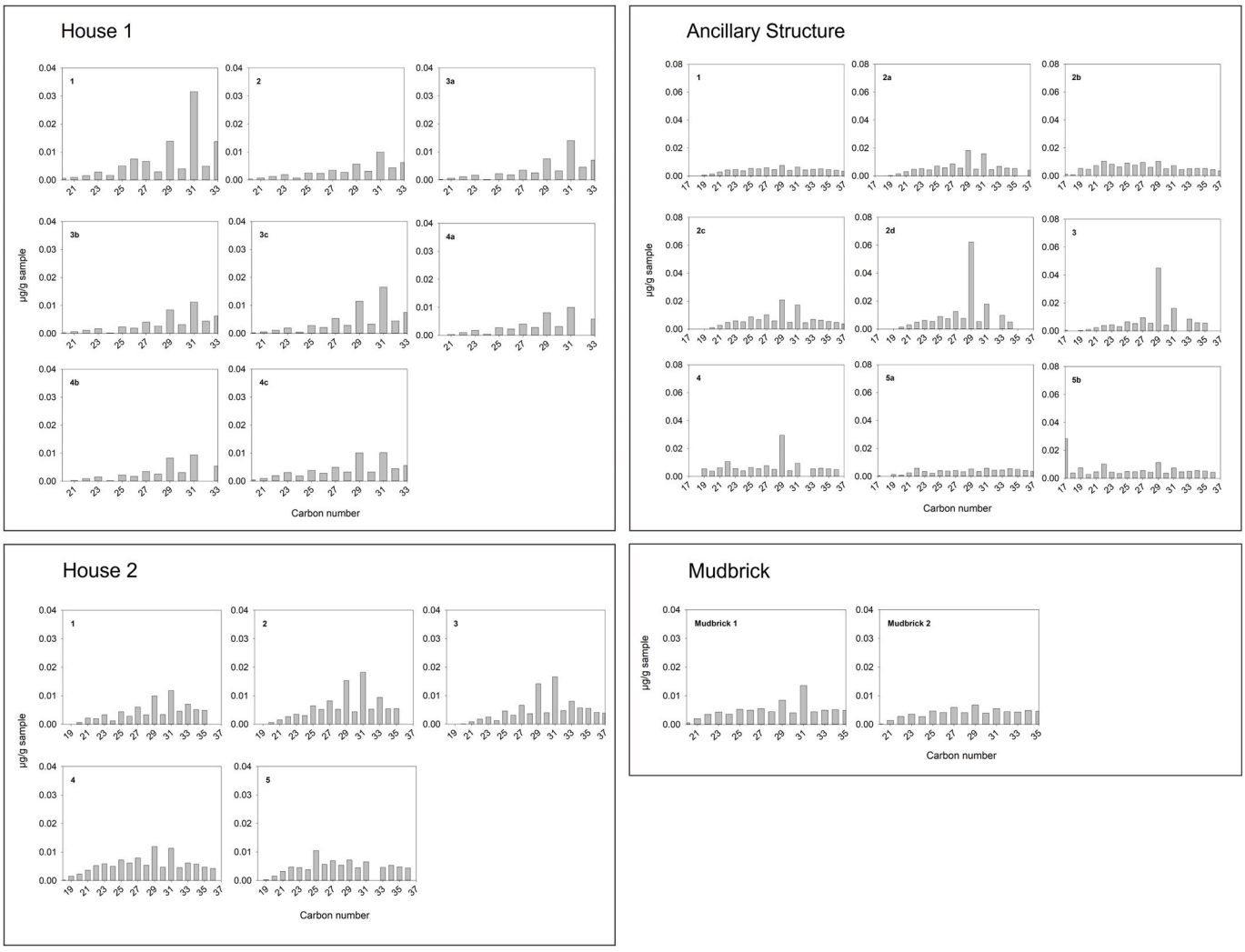

Fig. 7. Sedimentary *n*-alkane histograms from House 1, House 2, Ancillary Structure and mudbrick samples. Overall, the dominant *n*-alkanes are nC_{29} and nC_{31}. Note the good preservation of most of the samples (particularly in House 1), shown by a clear odd-over-even predominance, *vs* the degraded, smoothed *n*-alkane profiles displayed in the Ancillary Structure (specially in samples 5a and 5 b) and House 2 (sample 5).

features suggest that fire was utilized, most likely in the central clay hearth of House 1. However, it is important to note that these traces of past human activities are relatively scarce and are only present in specific sections of the sequence. The extensive maintenance carried out within the dwellings likely resulted in the removal of most anthropogenic components that were once deposited on the floors. This can be attributed to the frequent and intensive use of the buildings by their inhabitants (Schiffer, 1983).

However, despite the limited presence of anthropogenic micromorphological remains, the analysis of preserved lipids in the three sequences presents valuable potential for evaluating functionality. Notably, House 1, House 2, and the Ancillary Structure exhibit similar lipid profiles throughout their respective sequences (see supplementary material, Fig. 7 and Fig. 9). These include terpenoids (such as diterpenoids and triterpenoids), cholesterol and other sterols, oleic acid, as well as short and mid-chain alcohols and fatty acids (see supplementary material). Although the overall lipid profile of the sequences is homogeneous, diachronic variations in lipid content can be observed in all three cases (Fig. 9). For instance, in House 1, oleic acid is documented only in some of the layers, while dehydroabietic acid, a specific pyromarker found in burnt coniferous wood (Mackenzie et al., 1982; Oros and Simoneit, 2001a) and likely related to fuel use for fire, is consistently documented throughout the sequence. Besides variations in the *input* of oleic acid, the recurring presence of cholesterol and other sterols is also documented. This suggests that, in addition to the fuel *input*, activities performed inside the dwelling are generating a recurrent lipid residue, whose profile seems to be mostly linked to fats of plant origin (Brocks et al., 2003; Peters et al., 2007). It is important to note the lack of specific biomarkers exclusively associated with animal sources, as well as the absence of any micromorphological evidence indicating the presence of animal residues. Although we cannot precisely determine the original source (plant and/or animal) of these lipids in House 1, a high number of querns (17 fragments) have been documented inside the dwelling (Blanco-González et al., 2022), suggesting that this residue could be generated by such activity. Other significant archaeological artifacts, including oil lamps and pottery fragments (some of which are Phoenician and Egyptian in origin), were found in House 1 (Blanco-González et al., 2022). These items and/or the related activities that involved them could also be contributing lipids to the sediments within the house. However, the absence of diagnostic lipids and the scarce archaeological materials recovered inside the dwellings do not allow for further insights into the functionality of the space and its changes over time. The same residues appear in House 2, but the lipid residues from gymnosperm wood are present together with lipids specific to angiosperms (such as lupeol, olean-3-ene and β-Amyrin) (Diefendorf et al., 2012; Oros and Simoneit, 2001b), indicating a possible diachronic change in fuel use. This potential shift in fuel *input* could be related to the development of different activities inside the dwelling or a

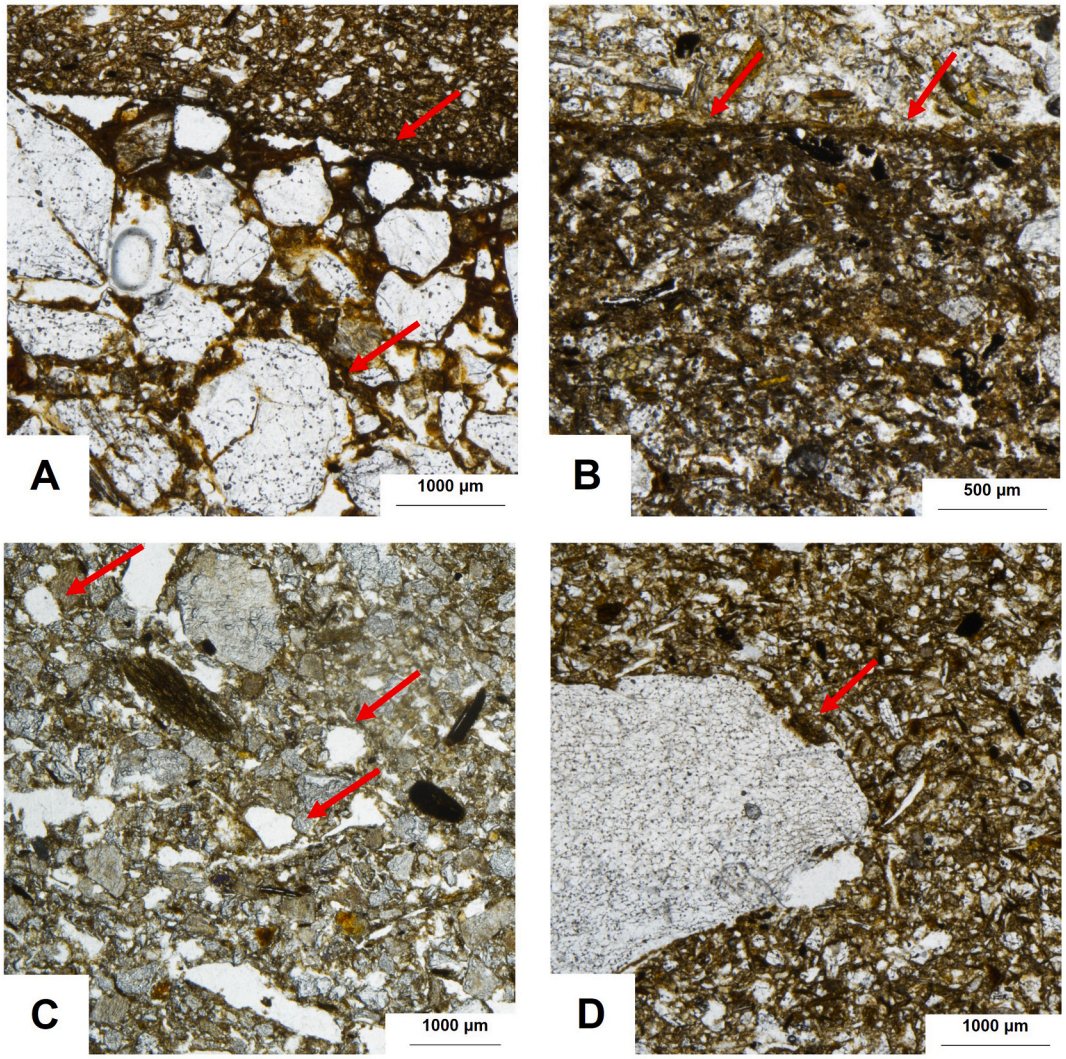

Fig. 8. Microphotographs (PPL) illustrating recurring micromorphological features in earth-based construction materials. A) House 1. Sharp contact between a floor preparation layer (MFT 1b) at the bottom, and a constructed clay floor on top (MFT 2a). The floor preparation layer (MFT 1b) displays recurrent clay coatings around the coarse quartz sand grains (arrow). Observe the well-defined clay lining (arrow) positioned atop the microfacies, precisely at the contact with the constructed clay floor (MFT 2a). B) House 1. Sharp contact between a constructed clay floor at the lower part (MFT 2a) and a floor preparation layer above (MFT 1a). Note the clearly defined clay lining (arrow) placed at the contact between the two microfacies. C) Mudbrick (MFT 5) displaying vughs and vesicles (indicated by arrows), the most prevalent porosity type in the analyzed earth-based construction materials at the site. D) Ancillary Structure. Constructed clay floor (MFT 2a) with a clay coating (arrow) encircling a coarse quartz sand grain. Notice the homogeneity of the surrounding groundmass, comprising dark brown undifferentiated silty-clay and fine-grained quartz and mica-type minerals. (For interpretation of the references to color in this figure legend, the reader is referred to the Web version of this article.)

diachronic change in fuel sourcing and/or use.

On the other hand, the Ancillary Structure presents a similar lipid *input* to that of House 1 and House 2, but it is richer in variety and quantity of compounds, particularly in fatty acids (see supplementary material, Fig. 9). Furthermore, throughout its sequence, both angiosperm and gymnosperm *inputs* are combined. However, the Ancillary Structure lacks domestic features (such as benches or combustion structures) and, moreover, it is too small to be a building intended for human occupation. In fact, these types of dwellings have been interpreted as granaries or spaces for storing agricultural-related products. Although the Ancillary Structure's lipid profile suggests the presence of plants rich in oils and fats that would have likely been deposited inside the structure, the low diagnostic value of the lipids and the absence of specific micromorphological features (i.e., seeds, phytoliths, burned plant remains) do not allow us to determine the specific product that was being stored, if that was indeed the functionality of the dwelling. It should be taken into account that no seeds or plant remains were either recovered inside the Ancillary Structure during its excavation. Possible ways to address the methodological limitations and data constraints of this study are discussed in the next section.

4.3. Advancing knowledge and future perspectives on early iron age Iberia

As part of our geoarchaeological microcontextual approach, we have successfully characterized three distinct types of construction layers within the domestic structures at Cerro de San Vicente, along with their associated cycles of use, renovation, and decay over time. Methodologically, we have conducted, for the first time in EIA contexts, the joint application of four high-resolution geoarchaeological techniques in a domestic village context. This study extends the groundwork laid by previous geoarchaeological research in the Iberian EIA (Belarte et al., 2023; Cutillas-Victoria et al., 2023; Mateu et al., 2013, 2019), contributing to our understanding of construction techniques, spatial utilization, and functional aspects of dwellings during this specific period. In fact, we have uncovered noteworthy similarities between the construction techniques employed at Cerro de San Vicente and those

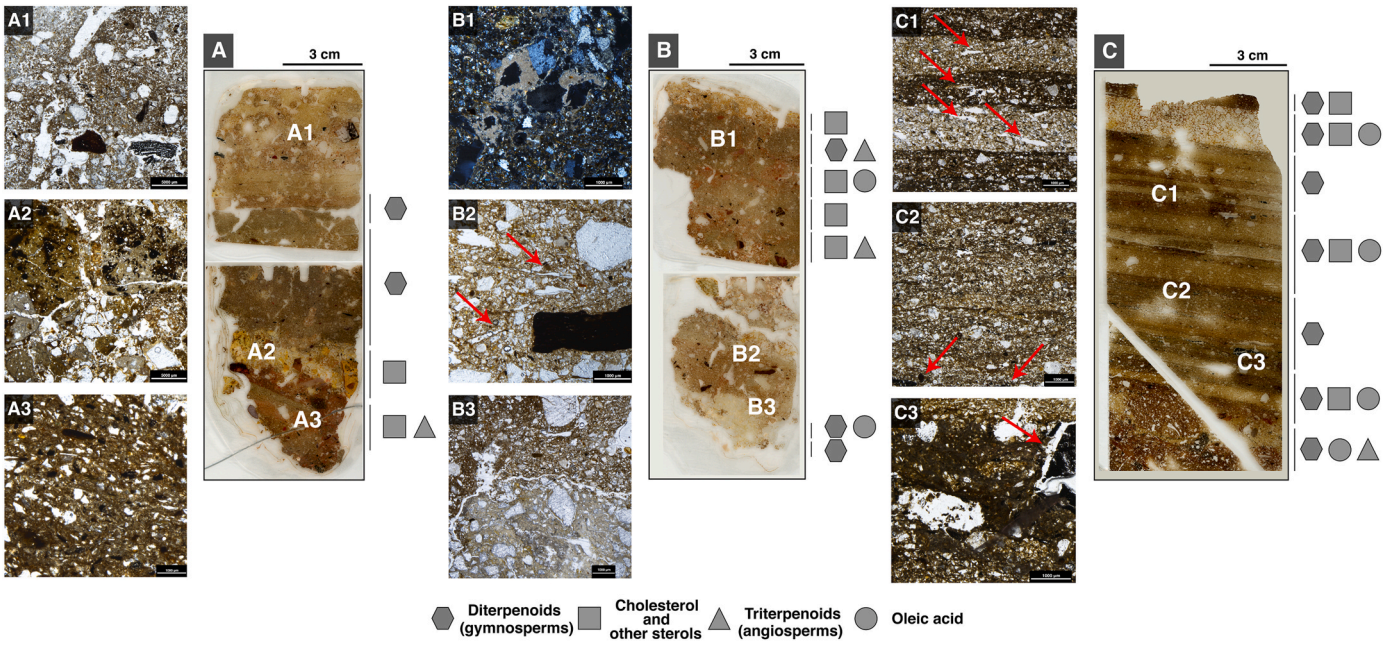

Fig. 9. Thin section scans from House 2 **(A)**, Ancillary Structure **(B)** and House 1 **(C)**, with microphotographs (in PPL, unless stated otherwise) showing features mentioned in the discussion and their interpretation. The gray icons represent major lipid compounds identified throughout the sequences. **A1**: MFT 3b. Decayed earthen construction material showing a channeled, bioturbated microstructure, disorthic clay nodules and angular charcoal fragments. **A2**: MFT 1b. Floor preparation layer, mainly composed of a light yellow, platy, silty-clayey micromass. **A3**: MFT 2a. Massive earthen floor, composed of dark brown silty-clay with fine quartz sand grains and a few slate fragments. The matrix is moderately well sorted and exhibits diffuse horizontal bedding, suggestive of an intentional mix. **B1**: MFT 3b. XPL. Decayed, bioturbated earthen construction material. Note the presence of carbonate hypocoatings around pores (vughs and chambers) indicative of post-depositional root action. **B2**: MFT 2a. Massive earthen floor, made of homogeneous brown clay mixed with quartz sand and slate fragments. Note the presence of diffuse subhorizontal bedding, vughs and subhorizontal moldic voids (arrows). **B3**: Sharp transition between a floor preparation layer (MFT 1b; lower part, massive light yellow silty-clayey deposit) and a massive earthen floor (MFT 2a; top part, massive dark brown silty-clayey deposit). **C1**: Succession of alternating light and dark brown, parallel horizontal, compact earthen floors (MFT 2a and MFT 2b) separated by sharp contacts. These exhibit subhorizontal bedding and moldic porosity (arrows). **C2**: MFT2b. Massive, dark brown earthen floor sequence exhibiting diffuse subhorizontal bedding and clay linings separating different floor deposits. Silt-sized rounded charred plant particles are present at the base (arrow). **C3**: MFT 4. Active organic-rich layer with charcoal fragments (arrow). (For interpretation of the references to color in this figure legend, the reader is referred to the Web version of this article.)

documented in the Mediterranean region of Iberia (Mateu et al., 2019). For example, in El Calvari del Molar, Mateu et al. (2019) identified earthen floors crafted using direct shaping techniques akin to those found in Cerro de San Vicente (MFT 2). Furthermore, they also observed the utilization of floor preparation layers for leveling purposes, similar in their features and composition to Cerro de San Vicente's MFT 3a. However, it is also important to acknowledge the existence of certain differences we encountered during our research. These include the presence of a distinct type of floor preparation layer at Cerro de San Vicente (MFT 1), variations in the thickness and recurrence of different construction layers, and the identification of distinct periods of abandonment and decay of the earthen material. By establishing these parallels and shedding light on regional variations, our findings significantly contribute to a broader comprehension of building traditions, their evolution, and continuity throughout the Iberian EIA.

Nevertheless, to obtain a more comprehensive understanding of construction techniques, space utilization, and daily life practices during the EIA in this region, further research is warranted. Firstly, it is crucial to expand the sampling of dwellings at Cerro de San Vicente for micromorphological and lipid analyses. In addition to sampling the floors, it is essential to include samples from the walls and other domestic elements such as benches and clay hearths. This broader sampling approach will provide deeper insights into construction techniques, raw material sourcing, and spatial organization within the village. Secondly, employing a more precise sampling technique, such as microdrilling of micromorphology blocks (Rodríguez et al., 2020), would be beneficial in the analysis of lipid biomarkers within complex earthen floor sequences. This approach aims to isolate lipids associated with specific microfacies, allowing for a more detailed examination of their composition and potential functional implications. Additionally, the implementation of compound-specific stable isotope analysis could offer valuable insights into the primary source of the lipids (Diefendorf et al., 2012; Jambrina-Enríquez et al., 2019; Peters et al., 2007), providing further understanding of the functionality and purpose of the dwellings. Furthermore, the application of μ-XRF and μ-XRD techniques could enhance the mineralogical characterization of each construction layer, providing more accurate and comprehensive data. By implementing these methodological advancements, future research endeavors will contribute to a more nuanced understanding of construction practices, raw material selection, and the multifaceted dynamics of daily life within the EIA settlement of Cerro de San Vicente.

From a broader perspective, acquiring geoarchaeological and microcontextual data from other EIA settlements in the Northern Iberian Plateau is essential to record site formation processes and to compare their construction techniques and the potential use and functionality of their dwellings with those of Cerro de San Vicente. This comparative analysis will contribute to a more comprehensive understanding of Cerro de San Vicente within its immediate archaeological context, shedding light on daily life practices and potential networks of influence and cultural exchange in the region. Moreover, it is crucial to compare the archaeological data from the Northern Iberian Plateau with that of other sites in EIA Iberia, allowing the placement of this region within a broader geographic and cultural framework. This comparative approach will provide insights into this period, characterized by population movements and the transmission of ideas, cultures, and skills between Iberia and other Mediterranean regions (Hodos, 2020).

5. Conclusions

In this geoarchaeological microcontextual study, we have conducted a comprehensive analysis of the intricate sequence of earthen floors within the domestic structures and dwellings of the best investigated quarter in an EIA village. Our research has revealed three distinct types of construction layers: clay floors, floor preparation layers, and decay deposits of earth-based construction material. We have documented cyclic patterns of use and maintenance in the dwellings, including regular replastering of the floors and cleaning activities. We have also documented phases of decay and abandonment in certain dwellings, which is remarkable as it challenges the misleading archaeological notion of simultaneous and continuous use of all buildings within a neighborhood. A more heterogeneous and intricate picture is now emerging, where inhabited and occupied buildings coexist alongside deserted and decaying structures. This observation aligns more closely with the expected dynamic cycle of household units within domestic contexts. Additionally, our research has identified abundant lipid biomarkers associated with these construction layers, which are potentially indicative of specific activities carried out within these dwelling spaces. The integration of high-resolution geoarchaeological techniques, such as soil micromorphology, lipid biomarker analysis, and XRD and XRF analysis, has provided precise insights into the deposits found in the EIA village of Cerro de San Vicente. These lines of evidence provide a solid foundation for moving beyond stagnant circular debates regarding the function and use of archaeological earthen architecture, which have relied solely on ethnological analogy. Our findings make a meaningful contribution to our understanding of construction techniques, daily life practices, and cultural traditions associated with building activities. They highlight the importance of the microcontextual, multi-technique approach in geoarchaeology and advance our knowledge of the EIA in the Northern Iberian Plateau.

Funding

This research was funded by the Spanish Ministry of Science and Innovation (Project PID 2019-104349 GA-I00, AEI/10.13039/501100011033) and a Gobierno de Canarias (ACIISI – Agencia Canaria de Investigación Innovación y Sociedad de la Información/Fondo Europeo de Desarrollo Regional "*Canarias Avanza con Europa*") predoctoral contract awarded to LT (TESIS2021010119).

Contributions

All authors have made substantial contributions to this study. **Laura Tomé**: Conceptualization, Formal analysis, Investigation, Writing - Original Draft, Visualization; **Eneko Iriarte**: Validation, Formal Analysis, Investigation, Resources, Writing - Review & Editing, Visualization; **Antonio Blanco-González**: Conceptualization, Resources, Writing - Review & Editing, Visualization, Supervision, Project administration, Funding acquisition; **Margarita Jambrina-Enríquez:** Validation, Writing - Review & Editing; **Natalia Égüez**: Validation, Writing - Review & Editing; **Antonio V. Herrera-Herrera**: Validation, Data Curation, Writing - Review & Editing; **Carolina Mallol**: Conceptualization, Validation, Formal Analysis, Investigation, Resources, Writing - Review & Editing, Visualization, Supervision.

Declaration of generative AI and AI-assisted technologies in the writing process

During the preparation of this work the authors used Chat GPT in order to improve English grammar of some parts of the text. After using this tool/service, the authors reviewed and edited the content as needed and take full responsibility for the content of the publication.

Declaration of competing interest

The authors have no competing interests to declare that are relevant to the content of this article.

Acknowledgements

This research paper is a component of LT's PhD thesis, and all authors are in agreement. The authors would like to thank Cristina Alario, Carlos Macarro and Juan Jesús Padilla for their field supervision, as well as the Cerro de San Vicente excavation team for their field work. We thank Jesús F. Jordá Pardo for his academic support in the early stages of this research and Javier Davara for helping with lab work. We thank Santiago Sossa Ríos for helping in the design and creation of the artwork. We are thankful to the CENIEH and I+D+i Scientific-Technological Center (Universidad de Burgos) personnel for thin section manufacture and mineralogical analyses (XRD and XRF), respectively. We thank Cristo Hernández, Alejandro Mayor, Santiago Sossa Ríos and Javier Davara for their comments and suggestions in an early version of the manuscript. Finally, we thank the anonymous reviewers who substantially contributed to improving this research paper.

Appendix A. Supplementary data

Supplementary data to this article can be found online at https://doi.org/10.1016/j.jas.2023.105897.

References

Albert, R.M., Lavi, O., Estroff, L., Weiner, S., Tsatskin, A., Ronen, A., Lev-Yadun, S., 1999. Mode of occupation of tabun cave, Mt carmel, Israel during the mousterian period: a study of the sediments and phytoliths. J. Archaeol. Sci. 26, 1249–1260. https://doi.org/10.1006/jasc.1999.0355.

Álvarez Sanchís, J.R., Lorrio Alvarado, A.J., Ruiz Zapatero, G., 2017. Los primeros elementos de hierro en Iberia. Anejos a Cuadernos De Prehistoria Y Arqueología 2, 149–161. https://doi.org/10.15366/ane2.blasco2016.012.

Álvarez-Sanchís, J.R., 2000. The iron age in western Spain (800 BC-ad 50): an overview. Oxf. J. Archaeol. 19, 65–89. https://doi.org/10.1111/1468-0092.00100.

Álvarez-Sanchís, J.R., Ruiz-Zapatero, G., 2014. The emergence of urbanism in early iron age central Iberia. In: Fernández-Gotz, M., Wendling, H., Winger, K. (Eds.), Paths to Complexity. Centralisation and Urbanisation in Iron Age Europe. Oxbow, Oxford, pp. 204–213.

Álvarez-Sanchís, J.R., Jimeno Martínez, A., Ruiz Zapatero, G., 2011. Aldeas y ciudades en el primer milenio a.C. La Meseta Norte y los orígenes del urbanismo. Complutum 22 (2).

Anderson, E., Almond, M.J., Matthews, W., 2014. Analysis of wall plasters and natural sediments from the Neolithic town of Çatalhöyük (Turkey) by a range of analytical techniques. Spectrochim. Acta Mol. Biomol. Spectrosc. 133, 326–334. https://doi.org/10.1016/j.saa.2014.04.072.

Arnaiz Alonso, M.Á., 2017. La I Edad del Hierro en la cuenca media del Duero: arquitectura doméstica y formas de poder político durante la Facies Soto (siglos IX-VII a.C.). Trab. Prehist. 74, 86–107. https://doi.org/10.3989/tp.2017.12185.

Belarte, M.C., Portillo, M., Mateu, M., Saorin, C., Pastor Quiles, M., Vila, S., Pescini, V., 2023. An interdisciplinary approach to the combustion structures of the Western Mediterranean Iron Age. the first results. J. Archaeol. Sci.: Rep. 47, 103803. https://doi.org/10.1016/j.jasrep.2022.103803.

Bellat, M., Baudouin, E., Cammas, C., Lyonnet, B., 2023. New insights into the Neolithic architecture of the Southern Caucasus: A micromorphological case-study from Mentesh Tepe (middle Kura Valley, Azerbaijan). J. Archaeol. Sci.: Report 49, 103971. https://doi.org/10.1016/j.jasrep.2023.103971.

Blanco-González, A., Padilla Fernández, J.J., Alario García, C., Macarro Alcalde, C., Dorado Alejos, A., Pazos García, R., Cerezo Fernández, R., Chapon, L., Sánchez Polo, A., 2022. Un santuario doméstico del siglo VII a. C. de culto a Hathor-Astarté en el Cerro de San Vicente (Salamanca, España). Trab. Prehist. 80, e06. https://doi.org/10.3989/tp.2023.12321 e06.

Blanco-González, A., 2011. From huts to "the house": the shift in perceiving home between the bronze age and the early iron age in central Iberia (Spain). Oxf. J. Archaeol. 30, 393–410. https://doi.org/10.1111/j.1468-0092.2011.00373.x.

Blanco-González, A., López-Sáez, J.A., 2013. Dynamics of pioneer colonisation in the early iron age in the Duero basin (central Iberia, Spain): integrating archaeological and palynological records. Environ. Archaeol. 18, 102–113. https://doi.org/10.1179/1461410313Z.00000000025.

Blanco-González, A., Alario García, C., Macarro Alcalde, C., 2017. The earliest villages in iron age Iberia (800-400 BC): a view from Cerro de San Vicente (Salamanca, Spain). Documenta Praehistorica 44, 386.

Blanco-González, A., Fernández Padilla, J.J., Alario García, C., Macarro Alcalde, C., Alarcón García, E., Martín Seijo, M., Chapon, L., Iriarte, E., Pazos García, R., Sanjurjo

Sánchez, J., Dorado Alejos, A., Tomé, L., Mallol, C., García Redondo, N., Carrancho, Á., Calvo Rathert, M., 2022. Un singular ambiente doméstico del Hierro I en el interior de la península ibérica: la casa 1 del Cerro de San Vicente (Salamanca, España). Trab. Prehist. 79, 346–361. https://doi.org/10.3989/tp.2022.12303.
Blanco-González, A., Padilla-Fernández, J.J., Dorado-Alejos, A., 2023b. Antiquity Mobile craftspeople and orientalising transculturation in seventh-century BC Iberia 97 (394), 908–926. https://doi.org/10.15184/aqy.2023.96.
Boivin, N., 2000. Life rhythms and floor sequences: excavating time in rural Rajasthan and Neolithic Catalhoyuk. World Archaeol. 31, 367–388. https://doi.org/10.1080/00438240009696927.
Brocks, J.J., Summons, R.E., Schlesinger, W., 2003. Sedimentary hydrocarbons, biomarkers for early life. Treatise on Geochemistry 8, 63–115. https://doi.org/10.1016/b0-08-043751-6/08127-5.
Cammas, C., 2018. Micromorphology of earth building materials: toward the reconstruction of former technological processes (Protohistoric and Historic Periods). Quat. Int. 483, 160–179. https://doi.org/10.1016/j.quaint.2018.01.031.
Cereda, S., Draganits, E., 2022. Lived monuments: a microarchaeological study of monumental architecture in the tell-site of Arslantepe (Malatya, Turkey). J. Archaeol. Sci.: Report 41, 103318. https://doi.org/10.1016/j.jasrep.2021.103318.
Cereda, S., Fragnoli, P., 2021. Petrography and micromorphology face-to-face: the potential of multivocality in the study of earth-based archaeological materials. Interdiscip. Archaeol. XII, 9–18. https://doi.org/10.24916/iansa.2021.1.1.
Connolly, R., Jambrina-Enríquez, M., Herrera-Herrera, A.V., Vidal-Matutano, P., Fagoaga, A., Marquina-Blasco, R., Marin-Monfort, M.D., Ruiz-Sánchez, F.J., Laplana, C., Bailon, S., Pérez, L., Leierer, L., Hernández, C.M., Galván, B., Mallol, C., 2019. A multiproxy record of palaeoenvironmental conditions at the Middle Palaeolithic site of Abric del Pastor (Eastern Iberia). Quat. Sci. Rev. 225, 106023 https://doi.org/10.1016/j.quascirev.2019.106023.
Courty, M.A., 2001. Microfacies analysis assisting archaeological stratigraphy. In: Goldberg, P., Holliday, V.T., Reid Ferring, C. (Eds.), Earth Sciences and Archaeology. Springer US, pp. 205–239. https://doi.org/10.1007/978-1-4615-1183-0_8.
Courty, M.A., Goldberg, P., Macphail, R., 1989. Soils and Micromorphology in Archaeology. Cambridge University Press.
Cutillas-Victoria, B., Lorenzon, M., Yagüe, F.B., 2023a. Earthen architecture and craft practices of early iron age ramparts: geoarchaeological analysis of Villares de la Encarnación, South-Eastern Iberia. Open Archaeol. 9 https://doi.org/10.1515/opar-2022-0304.
Cunliffe, B.W., Keay, S.J., 1995. Social Complexity and the Development of Towns in Iberia: from the Copper Age to the Second Century AD. British Academy.
Delibes de Castro, G., Romero Carnicero, F., 2011. La plena colonización agraria del Valle Medio del Duero. Complutum 22, 49–94.
Delibes de Castro, G., Romero Carnicero, F., Ramírez Ramírez, M.L., 1995. El poblado "céltico" de El soto de Medinilla (Valladolid). In: Delibes de Castro, G., Romero Carnicero, F., Morales, A. (Eds.), Arqueología Y Medio Ambiente. El Primer Milenio A.C. En El Duero Medio. Junta de Castilla y León, Valladolid, pp. 149–177.
Diefendorf, A.F., Freeman, K.H., Wing, S.L., 2012. Distribution and carbon isotope patterns of diterpenoids and triterpenoids in modern temperate C3 trees and their geochemical significance. Geochem. Cosmochim. Acta 85, 342–356. https://doi.org/10.1016/j.gca.2012.02.016.
Dietler, M., López-Ruiz, C., 2009. Colonial encounters in ancient Iberia: Phoenician, Greek, and indigenous relations. University of Chicago Press. https://doi.org/10.7208/chicago/9780226148489.001.0001.
Égüez, N., Dal Corso, M., Wieckowska-Lüth, M., Delpino, C., Tarantini, M., Biagetti, S., 2020. A pilot geo-ethnoarchaeological study of dung deposits from pastoral rock shelters in the Monti Sibillini (central Italy). Archaeol. Anthropol. Sci. 12, 114. https://doi.org/10.1007/s12520-020-01076-4.
Esparza Arroyo, Á., 2011. Los castros del oeste de la Meseta. Complutum 22, 11–47.
Fernández-Palacios, E., Jambrina-Enríquez, M., Mentzer, S., Rodríguez de Vera, C., Dinckal, A., Égüez, N., Herrera-Herrera, A.V., Navarro Mederos, J.F., Marrero Salas, E., Miller, C.E., Mallol, C., 2023. Reconstructing formation processes at the Canary Islands indigenous site of Belmaco Cave (La Palma, Spain) through a multiproxy geoarchaeological approach. Geoarchaeology. https://doi.org/10.1002/gea.21972.
Fernández-Posse, M.D., 1998. La investigación protohistórica en la Meseta y Galicia. Síntesis.
Freeman, K.H., Pancost, R.D., 2014. Biomarkers for terrestrial plants and climate. Treatise on Geochemistry 395–416. https://doi.org/10.1016/b978-0-08-095975-7.01028-7. Elsevier.
Friesem, D., Boaretto, E., Eliyahu-Behar, A., Shahack-Gross, R., 2011. Degradation of mud brick houses in an arid environment: a geoarchaeological model. J. Archaeol. Sci. 38, 1135–1147. https://doi.org/10.1016/j.jas.2010.12.011.
Friesem, D.E., Karkanas, P., Tsartsidou, G., Shahack-Gross, R., 2014a. Sedimentary processes involved in mud brick degradation in temperate environments: a micromorphological approach in an ethnoarchaeological context in northern Greece. J. Archaeol. Sci. 41, 556–567. https://doi.org/10.1016/j.jas.2013.09.017.
Friesem, D.E., Tsartsidou, G., Karkanas, P., Shahack-Gross, R., 2014b. Where are the roofs? A geo-ethnoarchaeological study of mud brick structures and their collapse processes, focusing on the identification of roofs. Archaeol. Anthropol. Sci. 6, 73–92. https://doi.org/10.1007/s12520-013-0146-3.
Friesem, D.E., Wattez, J., Onfray, M., 2017. Earth construction materials. In: Nicosia, C., Stoops, G. (Eds.), Archaeological Soil and Sediment Micromorphology, Wiley Blackwell. John Wiley & Sons, Oxford, pp. 99–110.
Friesem, D.E., Anton, M., Waiman-Barak, P., Shahack-Gross, R., Nadel, D., 2020. Variability and complexity in calcite-based plaster production: a case study from a Pre-Pottery Neolithic B infant burial at Tel Ro'im West and its implications to mortuary practices in the Southern Levant. J. Archaeol. Sci. 113, 105048 https://doi.org/10.1016/j.jas.2019.105048.
García-Redondo, N., Calvo-Rathert, M., Carrancho, Á., Goguitchaichvili, A., Iriarte, E., Blanco-González, A., Dekkers, M.J., Morales-Contreras, J., Alario-García, C., Macarro-Alcalde, C., 2021. Further evidence of high intensity during the Levantine iron age anomaly in southwestern Europe: full vector archeomagnetic dating of an early iron age dwelling from western Spain. J. Geophys. Res. Solid Earth 126. https://doi.org/10.1029/2021jb022614.
Gé, T., Courty, M.A., Matthews, W., Wattez, J., 1993. Sedimentary formation processes of occupation surfaces. In: Goldberg, P., Nash, D.T., Petraglia, M.D. (Eds.), Formation Processes in Archaeological Context. Prehistory Press, Madison, pp. 149–163.
Goldberg, P., Macphail, R.I., 2006. Practical and theoretical geoarchaeology. Blackwell Publishing. https://doi.org/10.1002/9781118688182.
Goldberg, P., Miller, C.E., Schiegl, S., Ligouis, B., Berna, F., Conard, N.J., Wadley, L., 2009. Bedding, hearths, and site maintenance in the middle stone age of sibudu cave, KwaZulu-natal, South Africa. Archaeol. Anthropol. Sci. 1, 95–122. https://doi.org/10.1007/s12520-009-0008-1.
Goodman-Elgar, M., 2008. The devolution of mudbrick: ethnoarchaeology of abandoned earthen dwellings in the Bolivian Andes. J. Archaeol. Sci. 35, 3057–3071. https://doi.org/10.1016/j.jas.2008.05.015.
Gutiérrez-Rodríguez, M., Brassous, L., Rodríguez Gutiérrez, O., Martín Peinado, F.J., Orfila, M., Goldberg, P., 2020. Site formation processes and urban transformations during Late Antiquity from a high-resolution geoarchaeological perspective: Baelo Claudia, Spain. Geoarchaeology 35, 258–286. https://doi.org/10.1002/gea.21769.
Herrera-Herrera, A.V., Mallol, C., 2018. Quantification of lipid biomarkers in sedimentary contexts: comparing different calibration methods. Org. Geochem. 125, 152–160. https://doi.org/10.1016/j.orggeochem.2018.07.009.
Herrera-Herrera, A.V., Mohamed-Rodríguez, N., Socas-Rodríguez, B., Mallol, C., 2020. Development of a QuEChERS-based method combined with gas chromatography-mass spectrometry for the analysis of alkanes in sediments. Microchem. J. 155, 104774 https://doi.org/10.1016/j.microc.2020.104774.
Hodos, T., 2020. The Archaeology of the Mediterranean Iron Age: a globalising world c.1100–600 BCE. Cambridge University Press. https://doi.org/10.1017/9780511979316.
Hoefs, M.J.L., Rijpstra, W.I.C., Sinninghe Damsté, J.S., 2002. The influence of oxic degradation on the sedimentary biomarker record I: evidence from Madeira Abyssal Plain turbidites. Geochem. Cosmochim. Acta. https://doi.org/10.1016/s0016-7037(02)00864-5.
Jambrina-Enríquez, M., Herrera-Herrera, A.V., Mallol, C., 2018. Wax lipids in fresh and charred anatomical parts of the Celtis australis tree: insights on paleofire interpretation. Org. Geochem. https://doi.org/10.1016/j.orggeochem.2018.05.017.
Jambrina-Enríquez, M., Herrera-Herrera, A.V., Rodríguez de Vera, C., Leierer, L., Connolly, R., Mallol, C., 2019. n-Alkyl nitriles and compound-specific carbon isotope analysis of lipid combustion residues from Neanderthal and experimental hearths: identifying sources of organic compounds and combustion temperatures. Quat. Sci. Rev. 222, 105899 https://doi.org/10.1016/j.quascirev.2019.105899.
Julivert, M., Fontboté, J.M., Ribeiro, A., Conde, L., 1972. Mapa tectónico de la Península Ibérica y Baleares, escala 1:1.000.000. Instituto Geológico y Minero de España, Madrid.
Karkanas, P., 2019. Microscopic deformation structures in archaeological contexts. Geoarchaeology 34, 15–29. https://doi.org/10.1002/gea.21709.
Karkanas, P., Efstratiou, N., 2009. Floor sequences in Neolithic Makri, Greece: micromorphology reveals cycles of renovation. Antiquity 83, 955–967. https://doi.org/10.1017/S0003598X00099270.
Karkanas, P., Goldberg, P., 2018. Reconstructing Archaeological Sites: Understanding the Geoarchaeological Matrix. John Wiley & Sons.
Karkanas, P., Brown, K.S., Fisher, E.C., Jacobs, Z., Marean, C.W., 2015. Interpreting human behavior from depositional rates and combustion features through the study of sedimentary microfacies at site Pinnacle Point 5-6, South Africa. J. Hum. Evol. 85, 1–21. https://doi.org/10.1016/j.jhevol.2015.04.006.
Leierer, L., Jambrina-Enríquez, M., Herrera-Herrera, A.V., Connolly, R., Hernández, C. M., Galván, B., Mallol, C., 2019. Insights into the timing, intensity and natural setting of Neanderthal occupation from the geoarchaeological study of combustion structures: a micromorphological and biomarker investigation of El Salt, unit Xb, Alcoy, Spain. PLoS One 14, e0214955.
Karkanas, P., Van de Moortel, A., 2014. Micromorphological analysis of sediments at the Bronze Age site of Mitrou, central Greece: patterns of floor construction and maintenance. J. Archaeol. Sci. 43, 198–213. https://doi.org/10.1016/j.jas.2014.01.007.
Leierer, L., Carrancho Alonso, Á., Pérez, L., Herrejón Lagunilla, Á., Herrera-Herrera, A.V., Connolly, R., Jambrina-Enríquez, M., Hernández Gómez, C.M., Galván, B., Mallol, C., 2020. It's getting hot in here–Microcontextual study of a potential pit hearth at the Middle Paleolithic site of El Salt, Spain. J. Archaeol. Sci. 123, 105237.
Lisá, L., Kočár, P., Bajer, A., Kočárová, R., Syrová, Z., Syrový, J., Porubčanová, M., Lisý, P., Peška, M., Ježková, M., 2020. The floor: a voice of human lifeways—a geo-ethnographical study of historical and recent floors at Dolní Němčí Mill, Czech Republic. Archaeol Anthropol Sci 12, 115. https://doi.org/10.1007/s12520-020-01060-y.
Lo Russo, S., Brönnimann, D., Deschler-Erb, S., Ebnöther, C., Rentzel, P., 2022. Mithraism under the microscope: new revelations about rituals through micromorphology, histotaphonomy and zooarchaeology. Archaeol. Anthropol. Sci. 14, 46. https://doi.org/10.1007/s12520-022-01505-6.
López-Sáez, J.A., Blanco-González, A., López-Merino, L., Ruiz-Zapata, M.B., Dorado-Valiño, M., Pérez-Díaz, S., Valdeolmillos, A., Burjachs, F., 2009. Landscape and climatic changes during the end of the late prehistory in the amblés valley (ávila,

central Spain), from 1200 to 400cal BC. Quat. Int. 200, 90–101. https://doi.org/10.1016/j.quaint.2008.07.010.
Lorenzon, M., 2021. From chaff to seagrass: the unique quality of Minoan mudbricks. A geoarchaeological approach to the study of architectural craft specialization in Bronze Age Crete. J. Archaeol. Sci.: Report 40, 103122. https://doi.org/10.1016/j.jasrep.2021.103122.
Lorenzon, M., Cutillas-Victoria, B., Holmqvist, E., Gkouma, M., Vrydaghs, L., Lichtenberger, A., Schreiber, T., Zardaryan, M., 2023. Exploring mudbrick architecture and its re-use in Artaxata, Armenia, during the 1st millennium BC. A multidisciplinary study of earthen architecture in the Armenian Highlands. PLoS One 18, e0292361. https://doi.org/10.1371/journal.pone.0292361.
Love, S., 2012. The geoarchaeology of mudbricks in architecture: a methodological study from Çatalhöyük, Turkey: geoarchaeology of mudbricks in architecture. Geoarchaeology 27, 140–156. https://doi.org/10.1002/gea.21401.
Macarro Alcalde, C., Alario García, C., 2021. Los orígenes de Salamanca. El poblado protohistórico del Cerro de San Vicente. Centro de Estudios Salmantinos.
Mackenzie, A.S., Brassell, S.C., Eglinton, G., Maxwell, J.R., 1982. Chemical fossils: the geological fate of steroids. Science 217, 491–504. https://doi.org/10.1126/science.217.4559.491.
Macphail, R.I., Goldberg, P., 2010. Archaeological materials. In: Stoops, G., Marcelino, V., Mees, F. (Eds.), Interpretation of Micromorphological Features of Soils and Regoliths. Elsevier, Amsterdam, pp. 589–622. https://doi.org/10.1016/B978-0-444-53156-8.00026-X.
Macphail, R.I., Goldberg, P., 2018. Applied Soils and Micromorphology in Archaeology, Cambridge Manuals in Archaeology. Cambridge University Press. https://doi.org/10.1017/9780511895562.
Massilani, D., Morley, M.W., Mentzer, S.M., Aldeias, V., Vernot, B., Miller, C., Stahlschmidt, M., Kozlikin, M.B., Shunkov, M.V., Derevianko, A.P., Conard, N.J., Wurz, S., Henshilwood, C.S., Vasquez, J., Essel, E., Nagel, S., Richter, J., Nickel, B., Roberts, R.G., Pääbo, S., Slon, V., Goldberg, P., Meyer, M., 2022. Microstratigraphic preservation of ancient faunal and hominin DNA in Pleistocene cave sediments. Proc. Natl. Acad. Sci. U. S. A. 119 https://doi.org/10.1073/pnas.2113666118.
Mateu, M., Bergadà, M.M., Garcia i Rubert, D., 2013. Manufacturing technical differences employing raw earth at the protohistoric site of Sant Jaume (Alcanar, Tarragona, Spain): construction and furniture elements. Quat. Int. 315, 76–86. https://doi.org/10.1016/j.quaint.2013.09.012.
Mateu, M., Bergadà, M.M., Armada, X.-L., Rafel, N., 2019. Micromorphology of the Early Iron Age semi-cemented floors: el Calvari del Molar (Tarragona, NE Spain) as case study. J. Archaeol. Sci.: Report 23, 746–762. https://doi.org/10.1016/j.jasrep.2018.11.028.
Mateu, M., Fernández, H., Daneels, A., Cabadas, H., Piña, S., 2022. Earthen architecture in the Mesoamerican classic period: a micromorphological approach to its manufacture process. J. Archaeol. Sci. 137, 105525 https://doi.org/10.1016/j.jas.2021.105525.
Matthews, W., French, C.A.I., Lawrence, T., Cutler, D.F., Jones, M.K., 1997. Microstratigraphic traces of site formation processes and human activities. World Archaeol. 29, 281–308. https://doi.org/10.1080/00438243.1997.9980378.
Milek, K.B., 2012. Floor formation processes and the interpretation of site activity areas: an ethnoarchaeological study of turf buildings at Thverá, northeast Iceland. J. Anthropol. Archaeol. 31, 119–137. https://doi.org/10.1016/j.jaa.2011.11.001.
Milek, K.B., Roberts, H.M., 2013. Integrated geoarchaeological methods for the determination of site activity areas: a study of a Viking Age house in Reykjavik, Iceland. J. Archaeol. Sci. 40, 1845–1865. https://doi.org/10.1016/j.jas.2012.10.031.
Nicosia, C., Stoops, G., 2017. Archaeological Soil and Sediment Micromorphology. Wiley Blackwell. John Wiley & Sons, Oxford.
Nicosia, C., Polisca, F., Miller, C., Ligouis, B., Mentzer, S., Mangani, C., Gonzato, F., 2022. High-resolution sediment analysis reveals Middle Bronze Age byre-houses at the site of Oppeano (Verona province, NE Italy). PLoS One 17, e0272561. https://doi.org/10.1371/journal.pone.0272561.
Nodarou, E., Frederick, C., Hein, A., 2008. Another (mud)brick in the wall: scientific analysis of Bronze Age earthen construction materials from East Crete. J. Archaeol. Sci. 35, 2997–3015. https://doi.org/10.1016/j.jas.2008.06.014.
Oros, D.R., Simoneit, B.R.T., 2001a. Identification and emission factors of molecular tracers in organic aerosols from biomass burning Part 1. Temperate climate conifers. Appl. Geochem. https://doi.org/10.1016/s0883-2927(01)00021-x.
Oros, D.R., Simoneit, B.R.T., 2001b. Identification and emission factors of molecular tracers in organic aerosols from biomass burning Part 2. Deciduous trees. Appl. Geochem. 16, 1545–1565. https://doi.org/10.1016/S0883-2927(01)00022-1.
Pastor Quiles, M., 2017. La construcción con tierra en Arqueología: Teoría, método, técnicas y aplicación. Universidad de Alicante.
Pastor Quiles, M., Knoll, F., Jover Maestre, F.J., 2019. ¿Adobes, terrones o bolas de barro amasado? Aportaciones para el reconocimiento arqueológico de las distintas técnicas constructivas que emplean módulos de tierra. Arqueología 25, 213–234. https://doi.org/10.34096/arqueologia.t25.n2.6868.
Peters, K.E., Walters, C.C., Moldowan, J.M., 2007. The Biomarker Guide: Biomarkers and Isotopes in the Environment and Human History. Cambridge University Press.
Rentzel, P., Nicosia, C., Gebhardt, A., Brönnimann, D., Pümpin, C., Ismail-Meyer, K., 2017. Trampling, poaching and the effect of traffic. In: Nicosia, C., Stoops, G. (Eds.), Archaeological Soil and Sediment Micromorphology. Wiley Blackwell, Oxford, pp. 281–297.
Rodríguez de Vera, C., Herrera-Herrera, A.V., Jambrina-Enríquez, M., Sossa-Ríos, S., González-Urquijo, J., Lazuen, T., Vanlandeghem, M., Alix, C., Monnier, G., Pajović, G., Tostevin, G., Mallol, C., 2020. Micro-contextual identification of archaeological lipid biomarkers using resin-impregnated sediment slabs. Sci. Rep. 10, 20574 https://doi.org/10.1038/s41598-020-77257-x.
Ruiz Zapatero, G., Álvarez-Sanchís, J.R., 2015. ¿Centros de poder? Sociedad y poblamiento en la Meseta Norte española (ca. 800 - 400 a.C.). Vegueta 15, 211–237.
Ruiz Zapatero, G., Álvarez-Sanchís, J.R., Rodríguez-Hernández, J., 2020. Urbanism in iron age Iberia: two worlds in contact. Journal of Urban Archaeology 1, 123–150. https://doi.org/10.1484/J.JUA.5.120913.
Schiffer, M.B., 1983. Toward the identification of formation processes. Am. Antiq. 48, 675–706. https://doi.org/10.2307/279771.
Shahack-Gross, R., Albert, R.-M., Gilboa, A., Nagar-Hilman, O., Sharon, I., Weiner, S., 2005. Geoarchaeology in an urban context: the uses of space in a Phoenician monumental building at Tel Dor (Israel). J. Archaeol. Sci. 32, 1417–1431. https://doi.org/10.1016/j.jas.2005.04.001.
Shillito, L.M., 2017. Multivocality and multiproxy approaches to the use of space: lessons from 25 years of research at Çatalhöyük. World Archaeol. 49, 237–259. https://doi.org/10.1080/00438243.2016.1271351.
Shillito, L.M., Matthews, W., 2013. Geoarchaeological investigations of midden-formation processes in the early to late ceramic neolithic levels at Çatalhöyük, Turkey ca. 8550-8370 cal BP. Geoarchaeology 28, 25–49. https://doi.org/10.1002/gea.21427.
Shillito, L.M., Ryan, P., 2013. Surfaces and streets: Phytoliths, micromorphology and changing use of space at Neolithic Çatalhöyük (Turkey). Antiquity 87 (337), 684–700. https://doi.org/10.1017/S0003598X0004939.
Shillito, L.M., Bull, I.D., Matthews, W., Almond, M.J., Williams, J.M., Evershed, R.P., 2011. Biomolecular and micromorphological analysis of suspected faecal deposits at Neolithic Çatalhöyük. Turkey. J. Archaeol. Sci. 38, 1869–1877. https://doi.org/10.1016/j.jas.2011.03.031.
Stahlschmidt, M.C., Miller, C.E., Kandel, A.W., Goldberg, P., Conard, N.J., 2017. Site formation processes and Late Natufian domestic spaces at Baaz Rockshelter, Syria: a micromorphological perspective. J. Archaeol. Sci.: Report 12, 499–514. https://doi.org/10.1016/j.jasrep.2017.03.009.
Stoops, G., 2003. Guidelines for analysis and description of soil and regolith thin sections. Soil Science Society of America.
Stoops, G., Canti, M.G., Kapur, S., 2017. Calcareous mortars, plasters and floors. In: Nicosia, C., Stoops, G. (Eds.), Archaeological Soil and Sediment Micromorphology, Wiley Blackwell. John Wiley & Sons, Oxford, pp. 189–199.
Sulas, F., Madella, M., 2012. Archaeology at the micro-scale: micromorphology and phytoliths at a Swahili stonetown. Archaeol. Anthropol. Sci. 4, 145–159. https://doi.org/10.1007/s12520-012-0090-7.
Tomé, L., Jambrina-Enríquez, M., Égüez, N., Herrera-Herrera, A.V., Davara, J., Marrero Salas, E., Arnay de la Rosa, M., Mallol, C., 2022. Fuel sources, natural vegetation and subsistence at a high-altitude aboriginal settlement in Tenerife, Canary Islands: microcontextual geoarchaeological data from Roques de García Rockshelter. Archaeol. Anthropol. Sci. 14, 195. https://doi.org/10.1007/s12520-022-01661-9.
Uzdurum, M., Schönicke, J., Kinzel, M., Barański, M.Z., 2023. Studying the use of earth in early architecture of southwest and central asia. Open Archaeol. 9 https://doi.org/10.1515/opar-2022-0321.
Villagran, X.S., Giannini, P.C.F., DeBlasis, P., 2009. Archaeofacies analysis: using depositional attributes to identify anthropic processes of deposition in a monumental shell mound of Santa Catarina State, southern Brazil. Geoarchaeology. https://doi.org/10.1002/gea.20269.